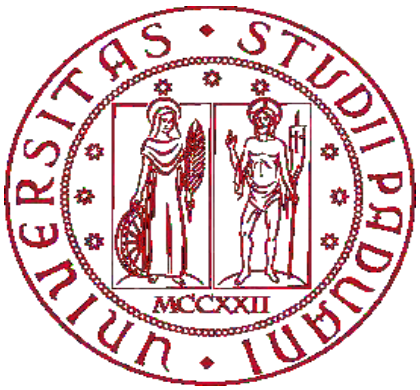

UNIVERSITÀ DEGLI STUDI DI PADOVA

Corso di Laurea Magistrale in Medicina e Chirurgia

Dipartimento di Salute della Donna e del Bambino

Clinica Ginecologica e Ostetrica

Direttore: Prof. Roberto Tozzi

TESI DI LAUREA

Innovative approaches in ovarian cancer treatment: The synergy of organoids and extracellular matrix in personalized medicine

Relatore: Prof. Carlo Saccardi

Correlatrice: Dott.ssa Giulia Spagnol

Laureanda: Shelly Michal Kotler

Matricola: 1178775

Anno Accademico 2023/2024

Index

ABSTRACT

Background

Ovarian cancer (OC) is regarded as a heterogeneous and malignant tumor type differentiated into various subtypes of which the high-grade serous ovarian cancer (HGSOC) is the most frequent and lethal. OC presents high mortality rates because of its nonspecific symptoms shown in the initial stages, absence of screening programs, and lack of knowledge regarding OC physiopathology. Treatment includes surgery and chemotherapy, but chemoresistance, especially in recurrent cases, poses a significant challenge. Currently, the most advanced in-vitro models are patient derived organoids (PDOs), three-dimensional constructs capable of mimicking tumor diversity. PDOs enable the analysis of patient-specific tumor properties and can therefore be employed to personalize therapeutic strategies. PDOs development requires a correct representation of the tumor microenvironment (TME) and the extracellular matrix (ECM). Cancer-associated fibroblasts (CAFs), are major regulators within the ECM, and significantly impact tumor proliferation, metastasis, and resistance to therapies by remodeling the ECM and influencing tumor-stromal interactions.

Purposes of the study

This study aims to successfully derive, culture, and characterize CAFs to enhance our understanding of the ECM and investigate the interactions between CAFs and tumor cells focusing on their impact on cell characteristics and proliferation.

Materials and Methods

CAFs were isolated and cultured from HGSOC samples, and their identity was confirmed using both bright-field microscopy and immunofluorescence (IF). Key markers such as CD29, FAP, and α-SMA were used to characterize the CAFs from the primary tumor and omental tissues. To evaluate their proliferation rate, Ki-67 staining was applied. Additionally, co-culture experiments with CAFs and the OVCAR3 cell line were carried out to investigate the interactions and proliferation of both cell types.

Results

CAFs were successfully derived and characterized from both primary tumor and omental samples, with positive expression of CD29, FAP, and α-SMA confirmed through IF analysis. Combined with the bright-field analysis, morphological differences were observed between the two populations, with omental CAFs exhibiting a rounded shape compared to the spindle-shaped primary tumor CAFs. Ki-67 proliferation analysis revealed 70% Ki-67 positive OVCAR3 cells, while CAFs showed a lower index of 5%, which slightly increased to 6.5% in the co-culture.

Conclusions

The derivation and culture of CAFs from HGSOC samples yielded viable cells, as confirmed by IF analysis, showing expected morphologies and positive expression of key markers. These findings suggest that our protocol, after further validation, could serve as a viable standardized method for CAFs derivation. Co-culture with OVCAR3 cells led to a slightly increased Ki-67 expression compared to CAFs cultured alone, suggesting a pro-proliferative interaction between the tumor cells and CAFs. This reinforces the importance of focusing on CAF-tumor interactions for developing improved models and therapeutic strategies.

RIASSUNTO

Presupposti dello studio

Il cancro ovarico (OC) è considerato una tipologia di tumore eterogeneo e maligno, suddiviso in vari sottotipi, tra i quali il carcinoma sieroso di alto grado (HGSOC) è il più frequente e letale. L'OC mostra alti tassi di mortalità a causa dei sintomi aspecifici nelle fasi iniziali, dell'assenza di programmi di screening e della mancanza di conoscenza riguardo alla fisiopatologia dell'OC. Il trattamento include chirurgia e chemioterapia, ma la chemioresistenza, specialmente nei casi ricorrenti, rappresenta una sfida significativa. Attualmente, i modelli in-vitro più avanzati sono gli organoidi derivati da paziente (PDOs), costrutti tridimensionali capaci di imitare la diversità tumorale. Gli PDOs permettono l'analisi delle caratteristiche tumorali specifiche del paziente e possono quindi essere utilizzati per personalizzare le strategie terapeutiche. Lo sviluppo dei PDOs richiede una corretta rappresentazione del microambiente tumorale (TME) e della matrice extracellulare (ECM). I fibroblasti associati al cancro (CAFs) sono importanti regolatori all'interno dell'ECM e influenzano significativamente la proliferazione tumorale, le metastasi e la resistenza alle terapie, rimodellando l'ECM e influenzando le interazioni tra il tumore e lo stroma.

Obiettivi dello studio

Questo studio mira a derivare, coltivare e caratterizzare con successo i CAFs per migliorare la comprensione dell'ECM e indagare le interazioni tra i CAFs e le cellule tumorali, concentrandosi sul loro impatto sulle caratteristiche cellulari e la proliferazione.

Materiali e metodi

I CAFs sono stati isolati e coltivati da campioni di HGSOC, e la loro identità è stata confermata utilizzando sia la microscopia a campo chiaro che l'immunofluorescenza (IF). Marcatori chiave come CD29, FAP e α-SMA sono stati utilizzati per caratterizzare i CAFs derivati dal tumore primario e dai tessuti omentali. Per valutare il loro tasso di proliferazione è stata applicata la colorazione con Ki-67. Inoltre, sono stati condotti esperimenti di co-coltura con CAFs e la linea cellulare OVCAR3 per indagare le interazioni e la proliferazione di entrambi i tipi.

Risultati

I CAFs sono stati derivati e caratterizzati con successo sia dai campioni del tumore primario che da quelli omentali, con espressione positiva di CD29, FAP e α-SMA confermata tramite analisi IF. Combinato con l'analisi a campo chiaro, sono state osservate differenze morfologiche tra le due popolazioni, con i CAFs omentali che mostravano una forma arrotondata rispetto ai CAFs del tumore primario, che erano a forma di fuso. L'analisi della proliferazione con Ki-67 ha rivelato un indice di proliferazione del 70% nelle cellule OVCAR3, mentre i CAFs hanno mostrato un indice inferiore del 5%, che è leggermente aumentato al 6,5% in co-coltura con le cellule tumorali.

Conclusioni

La derivazione e la coltura dei CAFs dai campioni di HGSOC hanno prodotto cellule vitali, come confermato tramite analisi IF, mostrando morfologie attese ed espressione positiva dei marcatori chiave. Questi risultati suggeriscono che il nostro protocollo, dopo ulteriori validazioni, potrebbe servire come un metodo standardizzato valido per la derivazione dei CAFs. La co-coltura con le cellule OVCAR3 ha portato a un leggero aumento del Ki-67 rispetto ai CAFs coltivati da soli, suggerendo un'interazione pro-proliferativa tra le cellule tumorali e i CAFs. Questo rafforza l'importanza di focalizzarsi sulle interazioni tra CAFs e tumore per sviluppare modelli e strategie terapeutiche migliorate.

Abbreviation Index

- **α-SMA**: Alpha-Smooth Muscle Actin
- **BRAF**: B-Raf Proto-Oncogene
- **BRCA1/2**: Breast Cancer Gene 1/2
- **CAFs**: Cancer-Associated Fibroblasts
- **CAR**: Chimeric Antigen Receptor
- **CAT**: Clot Activator Tube
- **CA125:** Cancer Antigen 125
- **CCC**: Clear-Cell Carcinoma
- **CD29**: Integrin Beta-1
- **CT**: Computed Tomography
- **CTNNB1**: Catenin Beta 1
- **DIL**: Dialkylcarbocyanine
- **DSBs**: Double-Strand Breaks
- **EC**: Endometrioid Carcinoma
- **ECM**: Extracellular Matrix
- **EMT**: Epithelial-Mesenchymal Transition
- **FAP**: Fibroblast Activation Protein
- **FBS**: Fetal Bovine Serum
- **FGF2**: Fibroblast Growth Factor-2
- **FIGO**: International Federation of Gynecology and Obstetrics
- **GEMMs**: Genetically Engineered Mouse Models
- **HE4:** Human Epididymis Protein 4
- **H&E**: Hematoxylin and Eosin
- **HGSOC**: High-Grade Serous Ovarian Carcinoma
- **HRD**: Homologous Recombination Deficiency
- **IF**: Immunofluorescence
- **Ki-67**: Marker for Cellular Proliferation

- **KRAS**: Kirsten Rat Sarcoma Virus
- **LGSOC**: Low-Grade Serous Ovarian Carcinoma
- **LOF**: Loss of Function
- **MC**: Mucinous Carcinoma
- **MRI:** Magnetic Resonance Imaging
- **OC**: Ovarian Cancer
- **PARP**: Poly (ADP-Ribose) Polymerase
- **PARPi**: Poly (ADP-Ribose) Polymerase inhibitors
- **PDGF**: Platelet-Derived Growth Factor
- **PDOs**: Patient-Derived Organoids
- **PDX**: Patient-Derived Xenografts
- **PET**: Positron Emission Tomography
- **P/S**: Penicillin-Streptomycin
- **PTEN**: Phosphatase and Tensin Homolog
- **ROCK**: Rho-Associated Kinase
- **SC**: Serous Carcinoma
- **TGF-β**: Transforming Growth Factor Beta
- **TME**: Tumor Microenvironment
- **TP53**: Tumor Protein P53
- **TVUS:** Transvaginal Ultrasound
- **WHO**: World Health Organization
- **2D**: Two-Dimensional
- **3D**: Three-Dimensional

1. INTRODUCTION

1.1. Ovarian cancer

Ovarian cancer (OC) is the leading cause of cancer related mortality in patients with gynecologic malignancies [1]. 70% of patients are diagnosed in stages III-IV [2] and the 5-year overall survival rate is around 51% [1,2,3].

OC is identified as either primary that arises from the ovarian tissue or secondary that develops from tissues that are extra-ovarian in origin. Primary OC comprises a number of histological types. Epithelial OC is the most prevalent, accounting for 95% of malignant cases [4]. The World Health Organization (WHO) also categorizes epithelial OC according to cell type which include: serous (SC), mucinous (MC), endometrioid (EC), and clear-cell carcinomas (CCC), as shown in Table I [5,6]. Non-epithelial cancers are rare, making up about 5% of all ovarian cancers. They are primarily germ cell and sex-cord stromal cancers, with small cell carcinoma and ovarian sarcoma occurring less frequently [7].

	Low-grade SC	High-grade SC	MC	EC	CCC
Frequency	<5%	70%	2–3%	10%	5–10%
Immunophenotype	CK7+,WT1+, ER+	CK7+, CK20, PAX8+, WT1+	CK7+, CK20–, ER–, PR–, WT1–	CK7+, PAX8+, CK20–, WT1–	napsin A+, WT1–, p53–, ER–
Precursor lesion	low-grade malignant potential lesions	STIC	borderline mucinous lesions	endometriosis	endometriosis
Molecular abnormalities	*KRAS, BRAF* [22, 23]	*TP53, BRCA1/2* [16, 17]	*KRAS, HER2* [5, 33–36]	*ARID1A, PTEN* [38]	*ARID1A, PIK3CA* [39, 51, 52]
Prognosis	intermediate	poor	good	favorable	intermediate

SC, serous carcinoma; MC, mucinous carcinoma; EC, endometrioid carcinoma; CCC, clear-cell carcinoma; STIC, serous tubal intraepithelial carcinoma; ER, estrogen receptor; PR, progesterone receptor.

***Table I*: Features of the 5 major subtypes of ovarian carcinoma.** *(Kossai et al. 2017)*

An additional classification system by the WHO, divides OC into two types according to their genetic and molecular profile. Type I tumors (80%) are slow growing and are associated with mutations in PTEN, BRAF, KRAS, CTNNB1, and PIK3CA. They include low-grade serous ovarian carcinoma (LGSOC), MC, EC,

malignant Brenner tumor, and CCC. Type II tumors (20%) present mutations in TP53 (96%), breast cancer gene 1 (BRCA1), breast cancer gene 2 (BRCA2), or CCNE1. They are aggressive with early metastases and include high-grade serous ovarian carcinoma (HGSOC) and carcinosarcoma. The penetration of these mutation varies based on family history and ethnicity and have higher frequencies in Ashkenazi jews. As a group, type II tumors are associated with a worse prognosis [7,8,9]. This classification is illustrated in Figure 1.

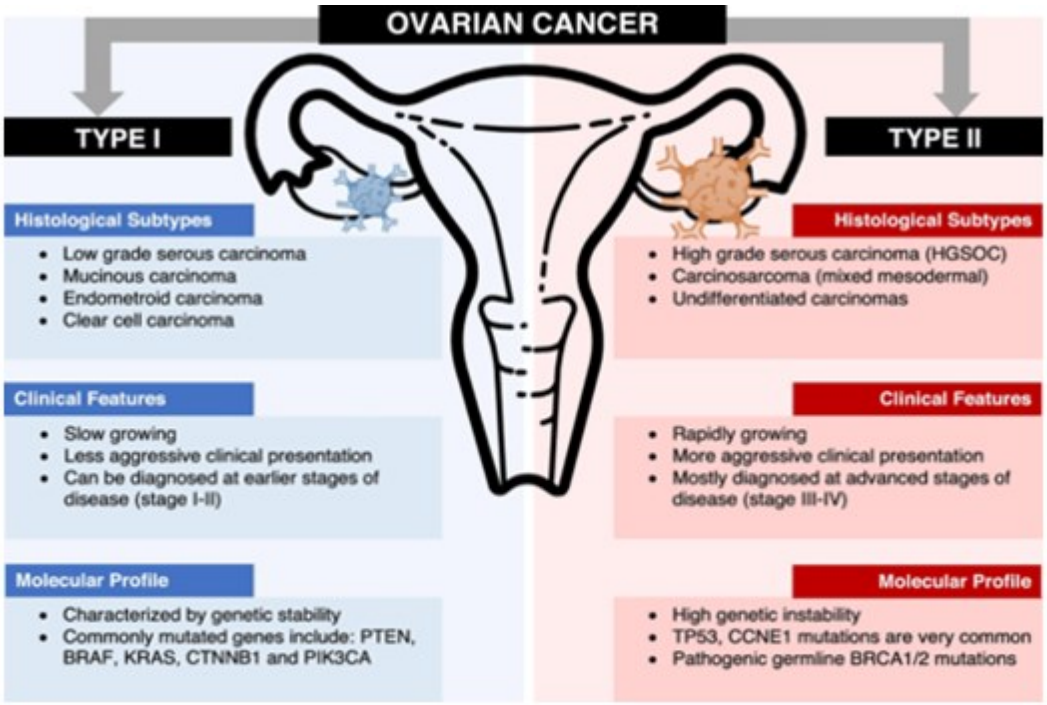

***Figure 1**: Schematic representation of ovarian cancer classification into type I and type II.* *(Zhu, Charkhchi, and Akbari 2022)*

OC is a multifactorial disease. While genetic mutations account for the majority of hereditary OC cases, there are other risk factors involved in the sporadic OC cases. These risk factors include increased ovulation cycles, such as those associated with early menarche, late menopause, and nulliparity. On the other hand, the use of combined estrogen-progestin contraceptive pills has been found to be protective[10].

Among women, OC is the sixth most frequent malignancy, accounting for 4% of all cancer-related deaths and ranking as the fifth leading cause of cancer death in

developed countries. It is more common in older than in younger women, with yearly diagnosis usually occurring around the age of 63, as seen in Figure 2 [11]. The highest prevalence of OC is listed in Western Europe and North America, with incidence rates ranging from 5 to 15 per 100,000 women, while lower rates are observed in the Middle East and Asia. These differences can be related to factors such as race, reproductive history, and lifestyle [12].

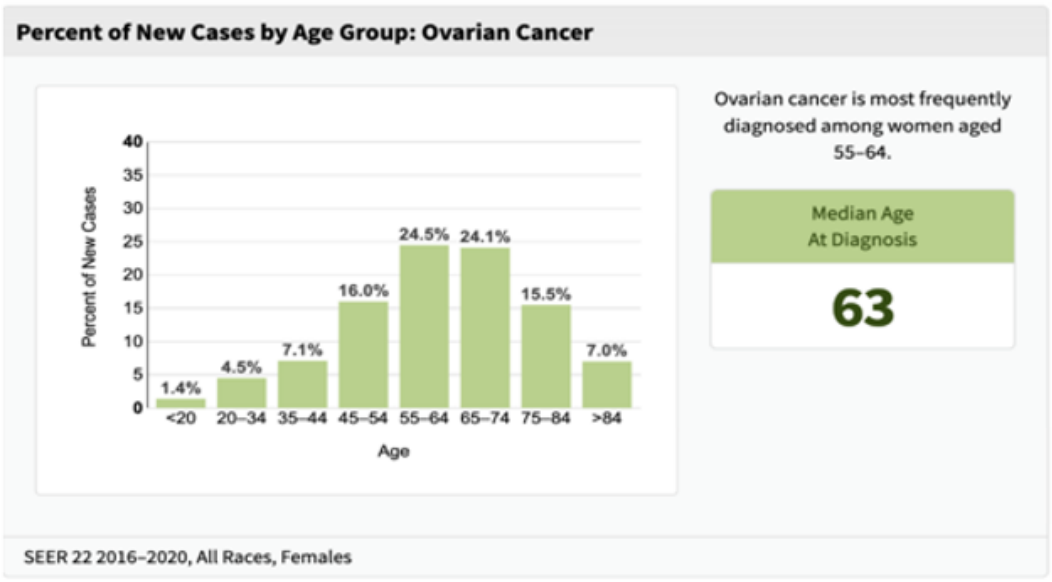

Figure 2: SEER cancer statistics factsheets on ovarian cancer. *(National Cancer Institute 2020)*

Since OC lacks specific symptoms which are often vague and non-specific, occurring only at advanced stages, early-stage diagnosis is rare. Possible symptoms include abdominal bloating, pain and changes in bowel habits [10].

OC diagnosis is done using a combination of imaging techniques such as transvaginal ultrasound (TVUS) combined with serum biomarkers including Cancer Antigen 125 (CA125) and Human Epididymis Protein 4 (HE4) [10,12]. For a definitive diagnostic confirmation, a tumor sample should be obtained either by TVUS-guided biopsy or during surgery for pathological analysis [10].

Computed tomography (CT) is the recommended imaging modality for staging OC and provides clinically relevant information including the size of the primary tumor, the size and localization of peritoneal implants and the status of lymph-

nodes, and is useful in evaluating response to treatment. Magnetic resonance imaging (MRI) is used for characterization of indeterminate lesions seen on CT or TVUS. Positron emission tomography (PET) and PET/CT are also helpful in staging OC and for detecting recurrent disease, especially in the setting of increasing tumor markers with negative imaging findings [13].

The main staging system employed for gynecologic tumors is the International Federation of Gynecology and Obstetrics (FIGO) staging system, that classifies the tumor in 4 stages according to its local and systemic progression, summarized in Table II. This classification system provides accurate prognostic information and guidance on the management of OC[14].

Stage	Extension
Stage I - Macroscopically limited to the ovaries	
Ia	One ovary is affected, capsule intact
Ib	Both ovaries are affected
Ic	Ia or Ib with tumor on the surface, broken capsule, ascites positive on cytological examination, or positive peritoneal washings
Stage II - Macroscopically limited to the pelvis	
Stage III - Abdominal disease and/or lymph nodes involved	
Stage IV - Disease spread beyond the abdomen	

Table II: The International Federation of Gynecology and Obstetrics (FIGO) tumor staging system.
(2014, Manuale di ginecologia e ostetricia)

Despite the high heterogeneous nature of OC, its treatment is standardized and primarily focused on radical surgical intervention followed by peritoneal washing and chemotherapy with platinum-based agents often in combination with taxanes. These agents work by damaging DNA or inhibiting cell division to prevent the cancer from spreading [15,16].

Chemotherapy response rate is around 80%. Unfortunately, after 2 years almost 70% of patients relapse and develop chemoresistance [17]. To address this challenge, targeted therapies and immunotherapy have been incorporated into the treatment arsenal in combination with chemotherapy and are used as maintenance therapy to reduce recurrence.

Poly (ADP-Ribose) Polymerase inhibitors (PARPi), for example, target cancer cells with specific genetic mutations (e.g. BRCA mutations) and have been shown to be effective in improving patient outcomes by preventing cancer cells from repairing their DNA, leading to apoptosis[16,18].

An innovative approach to overcoming resistance to therapy is personalized medicine that, based on the specific genetic characteristics of a patient's tumor, can predict the response to those treatments and improve their success potential[1,18,19].

1.1.1. High-Grade Serous Ovarian Carcinoma

HGSOC is the most common and lethal form of OC, known for its aggressive behavior and poor prognosis. This cancer typically originates from the epithelium of the fallopian tube and is often diagnosed at an advanced stage with over 70% of patients already exhibiting peritoneal dissemination [20]. In peritoneal dissemination cells detach from the primary tumor in the fallopian tube and spread with the peritoneal fluid to various sites within the peritoneal cavity. This results in a unique intra-abdominal environment that includes the primary tumor, peritoneal disseminations, omental metastasis and ascitic fluid [21]. This dissemination method is a distinctive feature of HGSOC, which does not encounter anatomical barriers that limit its dissemination.

HGSOC displays significant morphological diversity at both micro- and macroscopic levels, resulting from the tumor's metaplastic changes and differentiation processes. This diversity is traditionally categorized by examining Hematoxylin and

Eosin (H&E) stained morphologies, often in conjunction with molecular signatures[22]. The morphological characteristics can be classified into two distinct groups based on growth patterns seen in H&E. The first group is the classic feature group, which includes papillary, infiltrative micropapillary and papillary infiltrative growth patterns. The second group lacks the classic features and includes solid, pseudo-endometrioid and transitional growth patterns [23]. The patterns are illustrated in Figure 3.

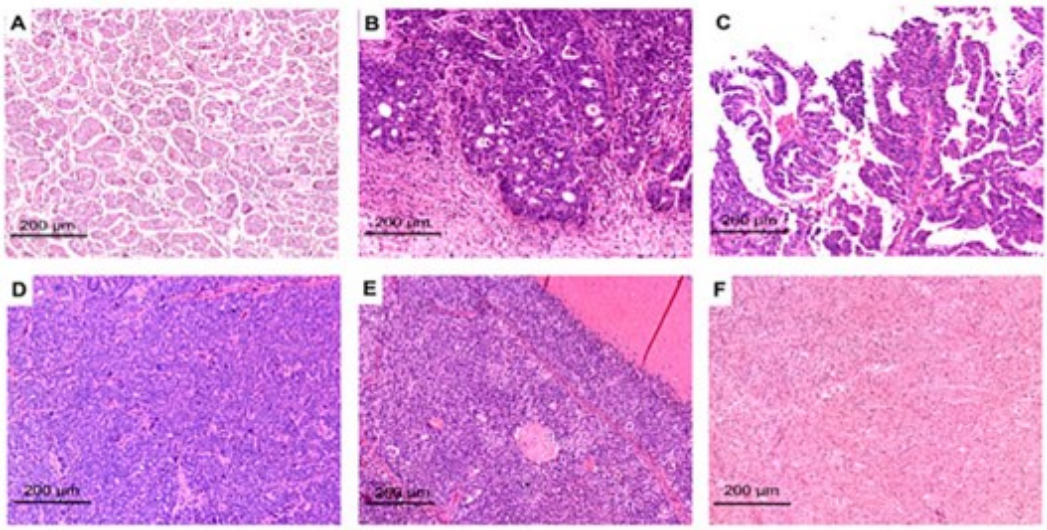

Figure 3: Representative H&E images of HGSOCs patterns. *(A) micropapillary, (B) pseudo-endometrioid, (C) papillary, (D) solid, (E) transitional-like, (F) healthy peritoneal fibrous tissue. (Azzalini et al. 2023)*

HGSOC is characterized by high levels of chromosomal instability. In 96% of cases, loss-of-function (LOF) mutations in TP53 can be found, which are critical to cancer pathogenesis [22,24]. Another frequent mutation is the LOF in the BRCA1 or BRCA2 gene, which leads to homologous recombination deficiency (HRD) [25]. PARPi exploits synthetic lethality in HRD-positive cells by trapping PARP1 at single-strand DNA breaks, leading to double-strand breaks (DSBs). In cells with BRCA1 or BRCA2 mutations, the inability to repair DSBs increases genomic instability and cell death, as shown in Figure 4. Therefore, HRD is a valuable biomarker for predicting PARPi therapy response in HGSOC, breast and prostate cancers[26].

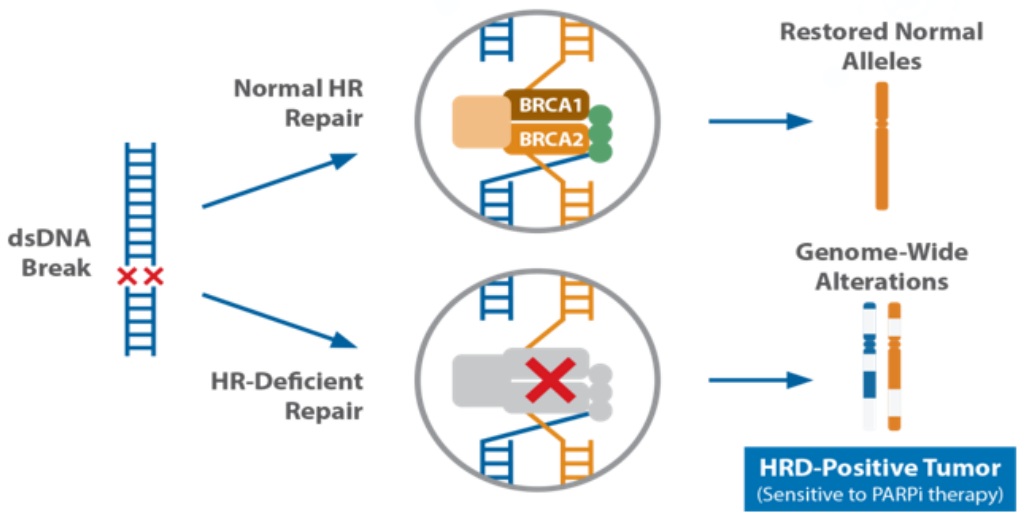

Figure 4: Homologous recombination deficiency (HRD). *(carislifescience.com/ Homologous recombination deficiency [HRD])*

The use of PARPi in HRD-positive HGSOC patients is a key example of the effectiveness of personalized medicine in addressing chemoresistance. To deepen our understanding of HGSOC biology and refine personalized therapies, preclinical cellular models are employed to mimic the in vivo environment.

Patient-derived organoids (PDOs) are three-dimensional (3D) models and are at the forefront of research in personalized medicine. They offer new ways to accurately simulate the tumor environment, test drugs more effectively, and gain deeper insights into the behavior of cancer cells under various treatment conditions[1,19]

1.2. Preclinical models for studying ovarian carcinoma

Even with advancements in OC treatment, only about 51% of patients survive for five years. This is mostly because there are no efficient screening programs in place and little knowledge of the distinct OC tumor biology [1,3], leading to worse prognosis and restricting the ability to personalize the therapy [7]. Enhancing the knowledge of cancer biology requires preclinical models that accurately reflect intra- and interpatient tumor heterogeneity [27]. As demonstrated in Figure 5, current preclinical models are divided into two-dimensional models (2D) such as cell lines, patient-derived xenografts (PDXs), genetically engineered mouse models (GEMMs) and 3D models, including spheroids, and PDOs [19].

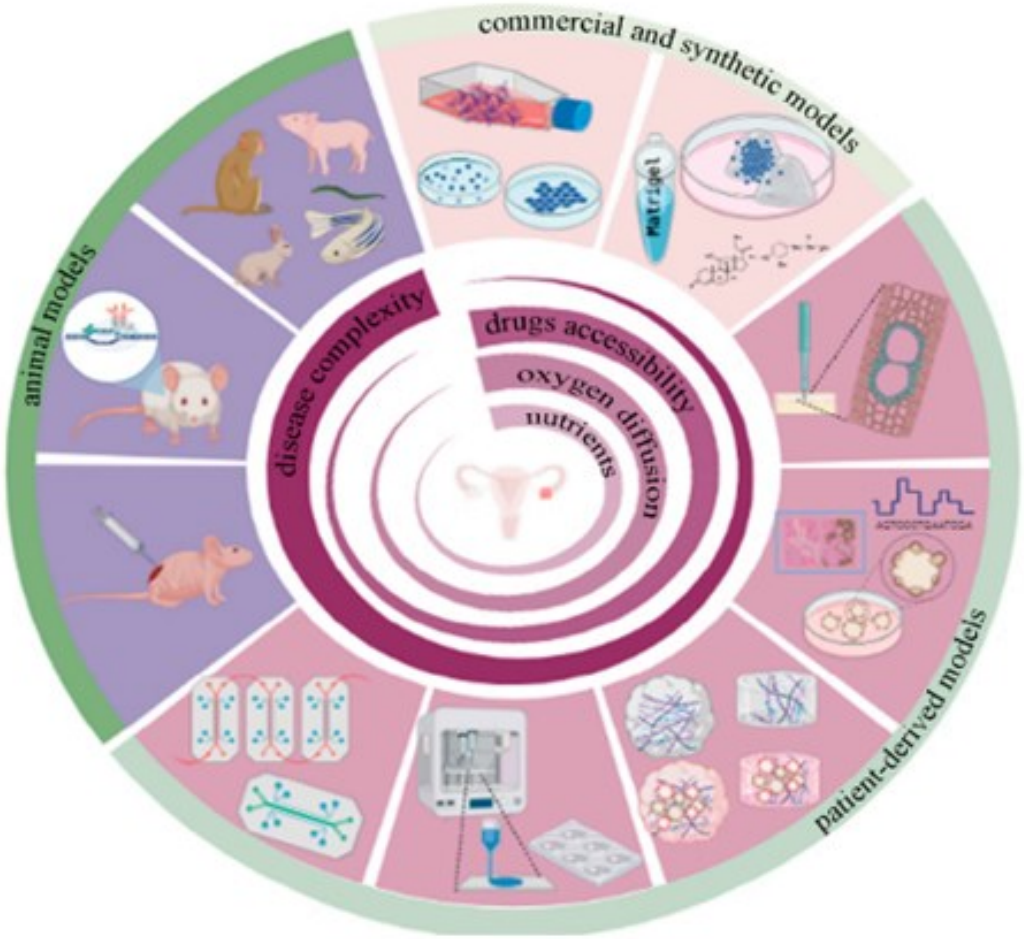

Figure 5: Preclinical models for epithelial ovarian cancer. *(Spagnol et al. 2023)*

Cancer cell lines are immortalized cells that can proliferate indefinitely in vitro. Because they are simple to use and easy to expand, they are frequently used for drug screening and identifying the histopathological subtypes of OC. However, the process of immortalizing primary tissue cell lines is highly inefficient, and extensive genetic shifts can occur during propagation, leading to significant alterations in morphology and biological properties [19,28]. Cell lines continue to be a widely used instrument for high-throughput drug screening despite these drawbacks.

PDXs are in vivo models created by implanting tumor tissues from patients into immunocompromised mice, preserving the original tumor's histological and genetic features. They provide a robust platform for drug testing, biomarker identification, tumor heterogeneity research and personalized medicine strategies development. However, challenges include potential loss of tumor heterogeneity over passages, clonal evolution, and the inability to replicate the human immune system. Additionally, the engraftment process can be time-consuming and not all tumor types engraft successfully [19,28].

GEMMs are mice genetically modified to carry mutations associated with human cancers, allowing them to mimic genetic alterations found in human tumors. These models are used for studying cancer development, progression and therapeutic strategies, as well as exploring cancer cell interactions with the tumor microenvironment (TME). However, GEMMs may not fully capture the complexity of human tumors due to the interspecies differences in the TME and immune responses. Furthermore, they take a long time to grow and might not correctly represent the heterogeneity seen in patient malignancies [19,29].

Spheroids are 3D models that provide a more realistic approach than 2D cultures. They allow cancer cells to grow in a manner that more closely mimics in vivo tumors. They can be formed from a single cell type or co-cultured with other cells. A few examples of this model's limitations are the variability in size and structure and the fact that they may not fully capture the complexity of actual tumors.

Despite these challenges, spheroids are essential tools for understanding tumor growth and researching new therapies [30,31].

PDOs are 3D tissue models that closely mimic in vivo tumors making them particularly valuable in personalized medicine. They maintain key characteristics such as genetic heterogeneity as well as nuclear and cellular atypia. They offer numerous clinical applications, including cancer and disease modeling, transcriptomics and epigenomic analysis, drug screening, toxicity testing and biobanking. Compared to other preclinical models, PDOs provide a more accurate representation of tumor behavior and are increasingly recognized as powerful tools in cancer research [27,32,33].

2D models are easy to use and cost-effective which makes them a popular tool in cancer research, but they are unable to replicate the complex TME and patient-specific tumor heterogeneity. On the other hand, 3D models, such as spheroids and PDOs, offer more realistic models, enhancing our ability to study cancer biology, cell-extracellular matrix interactions and develop personalized therapies[34,35].

1.3. Patient derived organoids

PDOs are 3D cell culture models derived from stem cells that replicate the architecture and functionality of real in-vivo tissue. They can be developed from various types of stem cells, including embryonic stem cells, pluripotent stem cells and adult progenitor stem cells (ASCs). Notably, PDOs are typically generated from ASCs specific to the epithelium of the organ in question, enabling them to closely mimic the morphology, mutational profile and gene expression patterns of the patient's original tumor [19].

PDOs preserve the complex cell-cell and cell-extracellular matrix interactions found in vivo, offering a more realistic environment than traditional 2D models. This allows PDOs to closely replicate human tissues, providing a valuable in vitro platform for studying human disease [36,37,38]. PDOs are more manageable compared to 2D models, such as PDXs. They can be established more efficiently from patient tissues, are less labor-intensive and are more scalable, making them an ethically favorable option for high-throughput drug screening and disease modeling [27,36].

Due to their promising potential as a preclinical drug screening platform in cancer research, researchers are creating PDO biobanks that could serve as a living repository that mirrors the diversity of patient tumors [39]. This biobanks will allow for high-throughput screening of drug libraries to identify potential therapeutic candidates [40,41].

There is preliminary evidence of the correlation between PDO drug screening results and clinical responses to systemic therapies and radiation [39]. Using these models to predict patient-specific drug response holds great promise as it could help clinicians in guiding personalized treatment decisions and optimizing patient outcomes [40].

However, PDOs are not without limitations. One significant challenge is the current inability to fully replicate the TME, which is essential for a complete physiological replication [36]. Efforts are ongoing to incorporate these elements into PDOs cultures to better model the TME and improve the relevance of these models in long-term culture and functional maturation. Another challenge is that, to accurately replicate a tumor, PDOs culture should contain only tumor cells, excluding healthy cells from the sample. The current solution for this challenge requires the use of selective media that can prevent the growth of non tumor-derived PDOs [42].

Additionally, optimizing PDOs establishment rates and reducing the time to obtain screening results is crucial to make this approach feasible [40,43]. Standardizing culture protocols and developing automated platforms can enhance reproducibility and throughput [40,41]. Lastly, integrating PDOs with advanced analytical techniques like image-based analysis can provide more comprehensive readouts of drug effects [40].

Despite these challenges, their potential is significant. PDOs are increasingly recognized as powerful tools for cancer research, drug discovery and personalized medicine as shown in Figure 6. With further optimization and clinical validation, PDO-based drug screening holds the potential to transform the cancer drug development process and improve outcomes for patients.

As the field progresses, it is anticipated that PDOs will play a central role in the future of precision oncology, bringing innovative techniques closer to clinical application. To further advance the development of accurate PDO models, correct representation and incorparation of all TME components is needed [36].

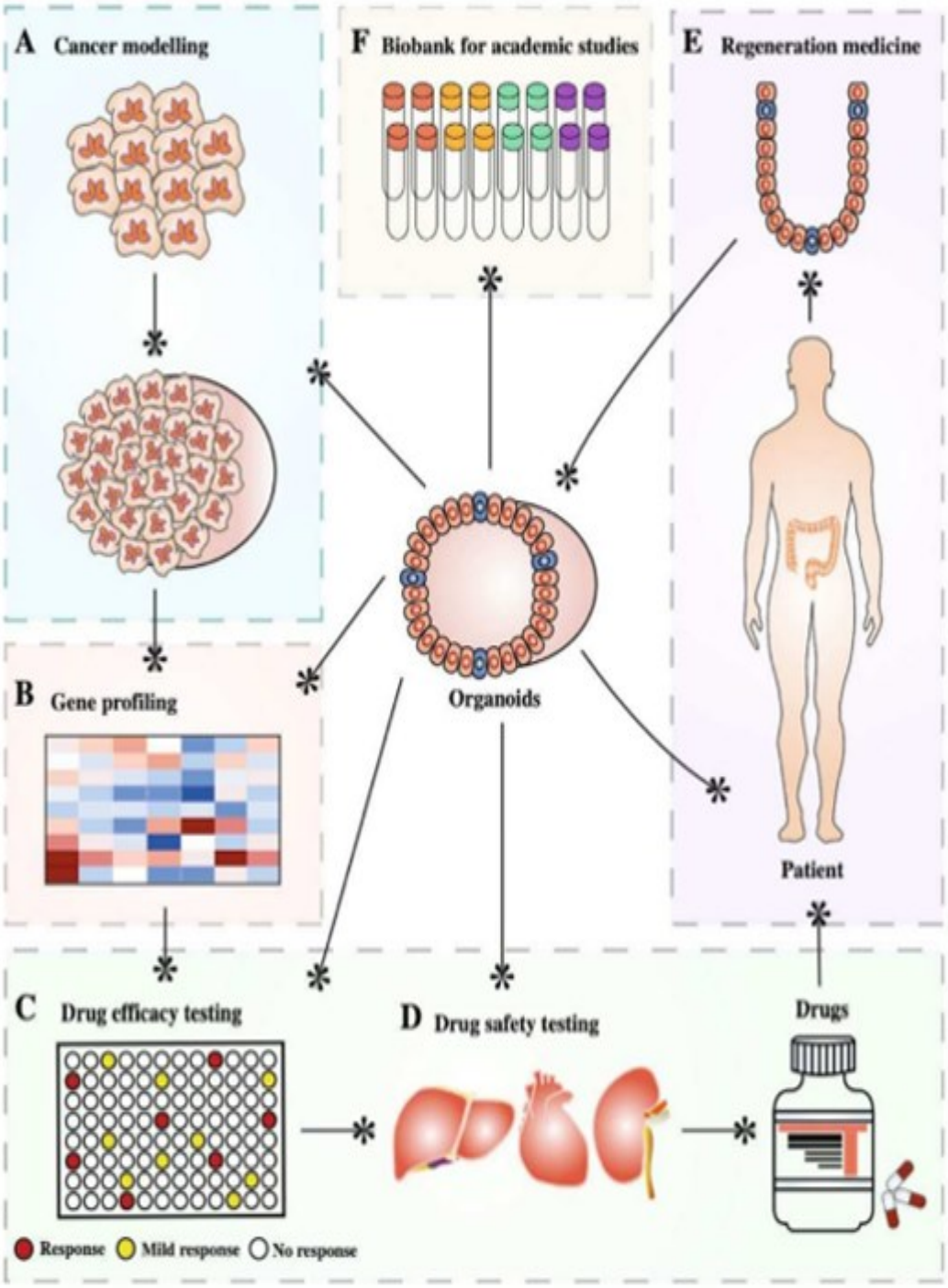

Figure 6: Potential applications of PDOs. (H. Xu et al. 2018)

1.4. Tumor microenvironment and extracellular matrix

The TME is the complex environment surrounding a tumor, including the extracellular matrix (ECM), blood vessels, immune cells, cancer-associated fibroblasts (CAFs), and signaling molecules, as demonstrated in Figure 7 [44,45].

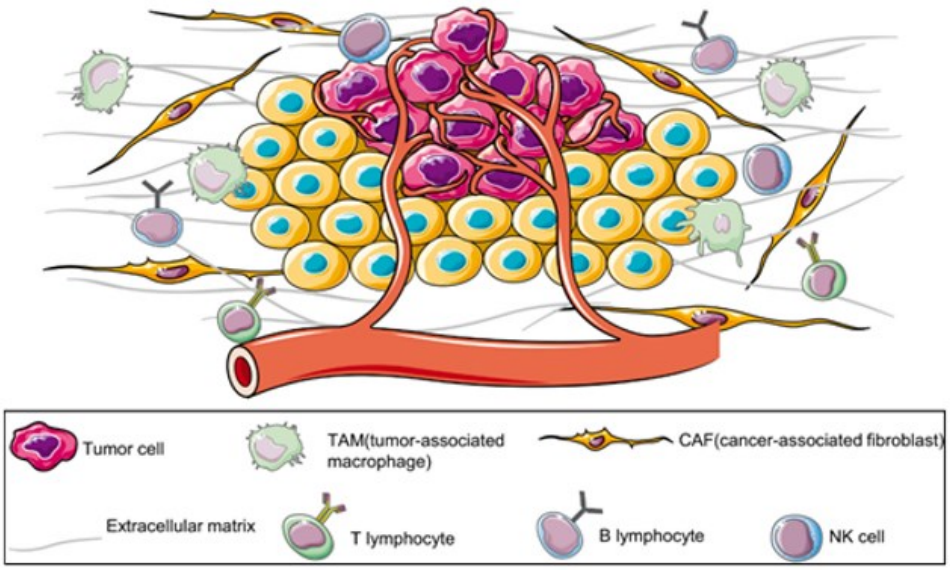

Figure 7: Tumor microenvironment components. *(Shi et al. 2024)*

This environment is not just a passive background for the tumor, as it actively participates in the tumor's progression and metastasis. Tumor cells can manipulate the TME to promote their survival, growth and invasion, making these interactions critical for understanding cancer biology and developing effective therapies [46,47]. To attest to that, targeting stromal cells within the TME has shown promise in enhancing chemotherapy efficacy and reducing tumor resistance [48].

The ECM is a vital component of the TME and serves as the scaffold that maintains tissue integrity and regulates cellular behavior through various biochemical signals. It is composed of a complex network of proteins and polysaccharides, such as collagen, elastin, fibronectin and laminin, that play crucial roles in cell adhesion, migration, differentiation and proliferation. Additionally, the ECM is dynamic, continuously undergoing remodeling to accommodate growth, development and repair processes [49].

ECM-based biomaterials are becoming increasingly utilized in medical research and therapeutic applications. For example, liver biomatrix derived from ECM of liver tissue has been shown to support hepatocyte culture better than traditional plastic substrates, retaining liver-specific functions for longer periods and highlighting the potential for tissue-specific ECM in regenerative medicine and tissue engineering [46].

In relation to PDOs, their development heavily relies on the ECM, as they require a supportive matrix that provides the necessary biochemical and physical signals for proper cellular organization and differentiation [50].

This can be explained by the fact that the ECM does not only support the mechanical structure of organoids, but also facilitates cellular signaling essential for the development of tissue-specific functions [19].

In cancer research specifically, tumor PDOs grown within an ECM scaffold can better replicate the heterogeneity and complexity of the original tumors, highlighting the value of exploring it [50]. The most commonly used type of ECM for cell culture matrix is Matrigel®, a solubilized basement membrane extracted from Engelbreth–Holm–Swarm mouse sarcoma, consisting of an undefined mixture of ECM proteins and growth factors. Geltrex™, another cell culture matrix, is interchangeable with Matrigel® but has less batch-to-batch composition and quality variation [51]. An alternative to Matrigel is ovarian tumor hydrogel, a peptide-protein co-assembling hydrogel-based multicellular 3D model for OC, which offers a more defined and reproducible matrix for organoid culture [52].

Among the components of the TME needed to develop accurate PDO models, CAFs are important, as they influence tumor progression, primarily through their influence on the ECM.

1.5. Cancer-associated fibroblasts

CAFs represent an importent and heterogeneous group of activated fibroblasts within the TME. Their presence and activity are fundamental in influencing cancer progression and metastasis, making them a major focus of oncological research and therapeutic development [53,54].

Elevated presence and density of CAFs within the TME are generally associated with poor prognosis [55]. This is primarily due to their role in promoting tumor progression and metastasis. Another role in worsening the prognosis, as demonstrated by Mhawech-Fauceglia et al., by increasing the resistance to platinum-based therapies as well as accelerating relapses in OC [56].

CAFs originate from diverse sources as demonstrated in Figure 8, the most common being resident fibroblasts within the tissue. Another common origin is from endothelial cells undergoing endothelial-mesenchymal transition (EMT) as tumors advance. Other possible origins are bone marrow-derived cells, mesenchymal stem cells and adipocytes [57]. This heterogeneity contributes to their functional diversity within the TME.

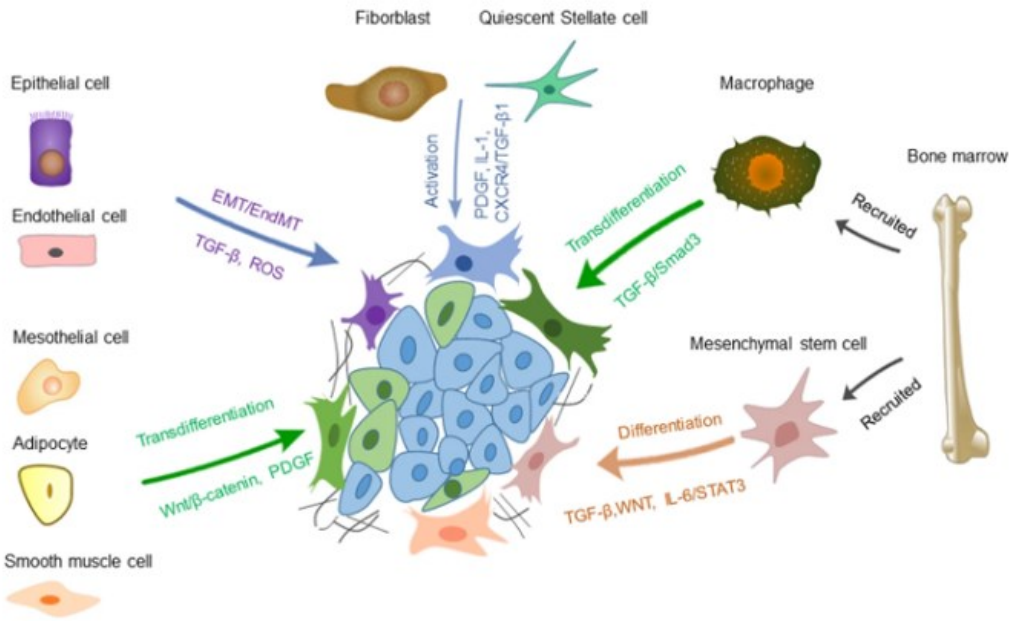

Figure 8: Multiple origins of CAFs and their potential precursor cells. *(Yang et al.2023)*

CAFs differ from resting fibroblasts in several key aspects. CAFs are generally larger, spindle-shaped and feature indented nuclei with branching cytoplasm. They exhibit enhanced proliferative, migratory and secretory abilities, making them more metabolically active than normal fibroblasts. They produce higher levels of ECM components such as tenascin (glycoprotein that support cellular adhesion and motility), periostin (protein that activates signaling pathways promoting cell survival, angiogenesis, invasion and EMT) and abnormally rigid collagen (structural protein necessary for tissue scaffolding, cell adhesion, migration and repair) [53,58-61].

The transition from resting fibroblasts to CAFs is driven by several signaling mechanisms, including Hippo pathway activation, LOF of TP53 and heat shock factor protein 1 activation. These mechanisms are often triggered by inflammation and changes in the ECM's structure and composition [53].

There are numerous markers available for identifying CAFs. The most promising ones, often considered specific "CAF markers" include fibroblast activation protein (FAP), α-smooth muscle actin (α-SMA) and integrin β1 (CD29). These markers have gained attention for their potential to accurately identify CAFs,

despite the inherent complexity and heterogeneity of fibroblast populations [53,62–64].

CAFs are critical players in tumor progression, primarily through their influence on the ECM within the TME. By employing both proteolytic and mechanical processes, CAFs modify the ECM's structure and stiffness, facilitating cancer cell migration and invasion as shown in Figure 9 [65]. By depositing new matrix components, CAFs not only supports tumor growth and metastasis but also creates physical barriers that impede drug delivery and immune cell infiltration [66]. In addition to these structural changes, CAFs secrete signaling molecules and ECM-degrading enzymes, further altering the TME to favor cancer progression [67].

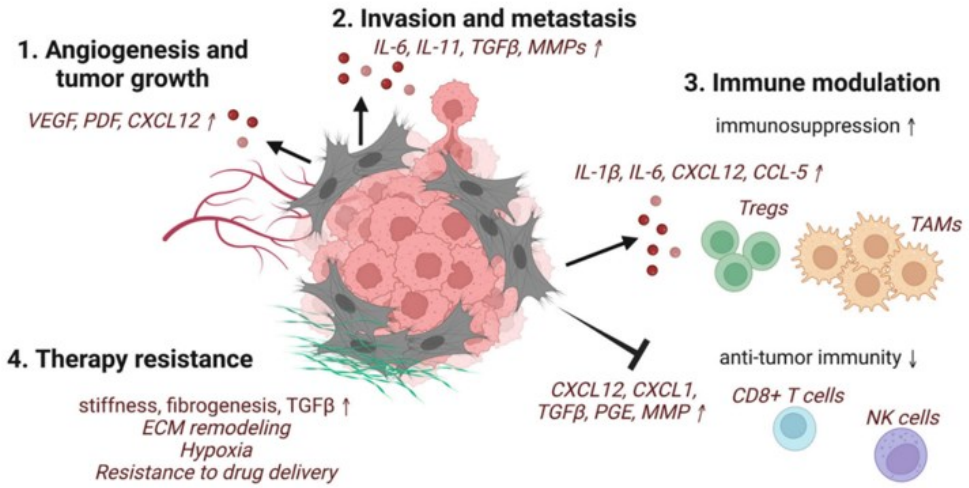

Figure 9: The mechanisms by which CAFs influence tumor progression. *(1) Angiogenesis and tumor growth, (2) Invasion and metastasis, (3) Immune modulation, (4) Therapy resistance.* (Glabman et al.2022)

Complementarily, tumor cells and other stromal cells within the TME also induce the conversion of fibroblasts into CAFs by releasing transforming growth factors, such as transforming growth factor beta (TGF-β), platelet-derived growth factor (PDGF) and fibroblast growth factor-2 (FGF2) [68].

The potential of targeting CAFs for cancer therapy has led to the exploration of various strategies, including CAF-targeted vaccines, Chimeric Antigen Receptor

(CAR) T cells and reprogramming CAF functions [53,65,66]. Nevertheless, the heterogeneity of CAFs, the lack of specific markers and the limitations of current animal models pose considerable challenges to these therapeutic approaches [57].

For PDOs, the interaction between CAFs and tumor cells within the ECM promotes a more relevant representation of the TME, enhancing the predictive power of the PDOs for drug screening and disease modeling. Furthermore, the presence of CAFs in PDO cultures can mimic the desmoplastic reaction often observed in tumors, providing insights into tumor progression and therapeutic responses. Thus, understanding the roles of CAFs, is essential for optimizing the design and application of PDOs in cancer research and regenerative medicine [57,69].

2. PURPOSES OF THE STUDY

The primary objectives of this study are as follows:

1. Establish a functional and reproducible protocol for the derivation and culture of CAFs from HGSOC, with the potential for future standardization.
2. Enhance our understanding of the ECM and investigate the interactions between CAFs and tumor cells, particularly focusing on their effects on cell behavior and proliferation.

3. MATERIALS AND METHODS

3.1. Patient population and inclusion criteria

Four biopsy samples were collected from HGSOC patients who underwent surgery at the Gynecologic and Obstetric Clinic of the University of Padua. The protocol received approval from ethics oversight institutions (Protocol Number P3059/2021).

All enrolled patients met the specified inclusion criteria, which were as follows:

- Histologically confirmed HGSOC
- Age > 18 years
- Written informed consent

3.2. Biopsy sample collection

Following collection, the biopsies were preserved in Tissue Storage Solution (MACS®, Miltenyi Biotech) combined with 1% P/S (Gibco™, Penicillins-Streptomycins) and 1% Anti-anti (Gibco™, Antibiotic-Antimycotic [100X]) before being transferred to the laboratory.

3.3. OVCAR3 cell cultures

OVCAR3 ovarian cancer cell lines were cultured in "Roswell Park Memorial Institute (RPMI) 1640 Medium" supplemented with 10% (v/v) fetal bovine serum (FBS), 1% (v/v) L-glutamine, and 1% (v/v) P/S solution. Cells were cultured in T75 cell culture flasks at 37°C with 5% CO2. For the co-culture experiment, the cells were plated in T75 flasks with DMEM medium. Upon reaching 85% confluence, cells were detached from the flasks using Trypsin-EDTA (0.025%) solution and subcultured in new flasks. The culture medium was changed every two to three days.

3.4. Derivation and culture of CAF

To generate CAFs from HGSOC samples, a protocol was established involving initial washing with a DMEM/F12-based buffer, followed by mechanical homogenization and enzymatic digestion using Liberase™ in a 24-well plate. After 1 hour of incubation at 37°C, the digestion was halted with a washing buffer, and the mixture was centrifuged. The pellet was filtered, washed and centrifuged again before being transferred to a T25 flask with culture medium. Cells were successfully cultured until 85% confluence, then detached with Trypsin-EDTA and subcultured. The medium was replaced every 48 hours. The full protocol can be found in the results chapter (4.2).

3.5. Immunofluorescence staining of CAFs

To conduct immunofluorescence (IF) imaging, the samples were fixed with 4% paraformaldehyde (PFA) for 10 minutes and then subjected to sucrose gradient treatment (10%, 15%, and 30%, each for 3 hours) at 4°C. The samples were permeabilized using a 0.5% (v/v) Triton X-100 solution in 1X PBS for 20 minutes at room temperature (RT) and subsequently washed with 1X PBS for 5 minutes. The sections were then blocked with 10% (v/v) horse serum in 1X PBS for 40 minutes at RT, followed by another 5-minute wash with 1X PBS at RT.

The samples were then incubated with the following primary antibodies: mouse anti-integrin β1/ITGB1, rabbit anti-fibroblast activation protein, and rabbit polyclonal anti Ki-67 diluted according to the specifications in Table III and stored in the dark at 4°C for 24 hours. A subsequent primary antibody goat anti-alpha smooth muscle actin was added, diluted as specified in Table III, and incubated for 2 hours at 37°C. The samples were then washed with 1X PBS at RT for 10 minutes.

Next, the samples were incubated with secondary antibodies: goat anti-mouse, goat anti-rabbit, donkey anti-goat and chicken anti-rabbit diluted as described in Table III, for 1 hour at 37°C in the dark. Following this, the samples underwent a

final wash with 1X PBS at RT, protected from light, for 10 minutes. Nuclei were stained at a dilution of 1:10000 HOECHST (Life Technologies) for 15 minutes at RT in the dark.

A last wash was performed in 1X PBS and cells were maintained in 1X PBS to be analyzed. Images were acquired with a fluorescence inverted microscope (Zeiss Axio Observer). Using ImageJ software, the number of Ki-67 positive cells divided by the number of total nuclei was calculated to quantify the number of proliferating cells.

Antibody	Producer and ref. number	Primary/ Secondary	Dilution
Mouse monoclonal anti-Integrin β1/ITGB1 (JB1B) antibody (CD29)	Santa Cruz biotechnology SC59829	Primary	1:50 in 1X PBS + 1% BSA
Rabbit Polyclonal anti Fibroblast activation protein (FAP) antibody	Arigo bio laboratories ARG66701	Primary	1:100 in 1X PBS + 1% BSA
Goat Polyclonal anti alpha smooth muscle actin antibody (α-SMA)	Arigo bio laboratories ARG63621	Primary	1:50 in 1X PBS + 1% BSA
Rabbit polyclonal anti-Ki67 antibody	ProteinTech, 27309-AP-1	Primary	1:100 in 1X PBS + 1% BSA
CoraLite488-conjugated Goat Anti-Mouse IgG(H+L)	ProteinTech, AB_2810983 Cat no : SA00013-1	Secondary	1:200 in 1X PBS + 1% BSA
CoraLite594 – conjugated Goat Anti-Rabbit IgG(H+L)	ProteinTech, AB_2810984 Cat no : SA00013-4	Secondary	1:200 in 1X PBS + 1% BSA
CF647 Donkey anti-goat IgG (H+L)	Biotium, Cat no:20048	Secondary	1:200 in 1X PBS + 1% BSA
Chicken anti-Rabbit IgG (H+L) Cross-Adsorbed Secondary Antibody, Alexa Fluor™ 488	Thermo Fisher Scientific, catalog # A-21441, RRID AB_2535859	Secondary	1:200 in 1X PBS + 1% BSA

Table III: Primary and secondary antibodies used for IF assays

3.6. Co-culture of OVCAR3 cell line and CAF

To create the co-cultures, 30.000 cells from OVCAR3 cell line and 30.000 cells from CAFs KOV71 were harvested in a 24-multiwell plate. Beforehand cells from the OVCAR3 cell line were stained with DIL dye (dilution 1:200 in PBS). The co-culture was resuspended in 800µl of DMEM supplemented with 10% (v/v) FBS, 1% (v/v) L-glutamine, and 1% (v/v) P/S solution. After 24 hours, co-culture was observed using a Zeiss Axio Observer microscope to assess the bidirectional interactions between CAFs and cancer cells.

3.7. Statistical analysis

All graphs and statistical analyses were performed using the GraphPad Prism Software 8.4. Data were expressed as means ± SE.

For the comparison between paired experimental groups, Student's t-test was used for parametric datasets, and the Mann-Whitney test was used for non-parametric datasets. p-value < 0.05 was considered statistically significant.

4. RESULTS

During the extraction of CAFs, we developed this derivation protocol for the establishment of CAFs biorepositories based on the "OC PDOs biorepository" protocol.

4.1. OC CAFs biorepository establishment protocol

1. **Sample collection:**
    - **a.** Perform OC surgery (laparoscopic or laparotomic) as per standard clinical procedures.
    - **b.** Place excised tissues on a sterile surface while wearing sterile gloves.
    - **c.** Under gynecologist supervision, identify the ovaries and the tumor site.
    - **d.** Using a sterile scalpel, excise a significant sample of ovarian tumor tissue (1.5-2 cm), avoiding necrotic or iatrogenically altered material.
    - **e.** Repeat the procedure to obtain a sample of normal tissue (preferably ovarian tissue; peritoneum or omentum may also be used if normal ovarian tissue is unavailable).
    - Additional biopsies of tumor or peritumoral tissues can be taken as necessary.
2. **Sample handling:**
    - **a.** Place each tissue sample into falcon tubes containing 10 mL of MACS® Tissue Storage Solution to cover the sample.
    - **b.** Label the test tube caps:
        - **i.** **T** for the tumor sample
        - **ii.** **N** for the normal tissue sample.
3. **Arterial blood sampling:**
    - **a.** Fill 3 vacutainers (6 mL each) with:

   i. 1 Clot activator tube (CAT) with a red cap for serum storage.
   ii. 2 K2EDTA tubes (K2E) with violet caps for plasma storage.

b. Mark all tubes with the patient's identification tag.

4. **Sample transport**: Transport the falcon tubes containing the biopsy in 10 mL of MACS® Tissue Storage Solution in an iced box.

The protocol is demonstrated in Figure 10.

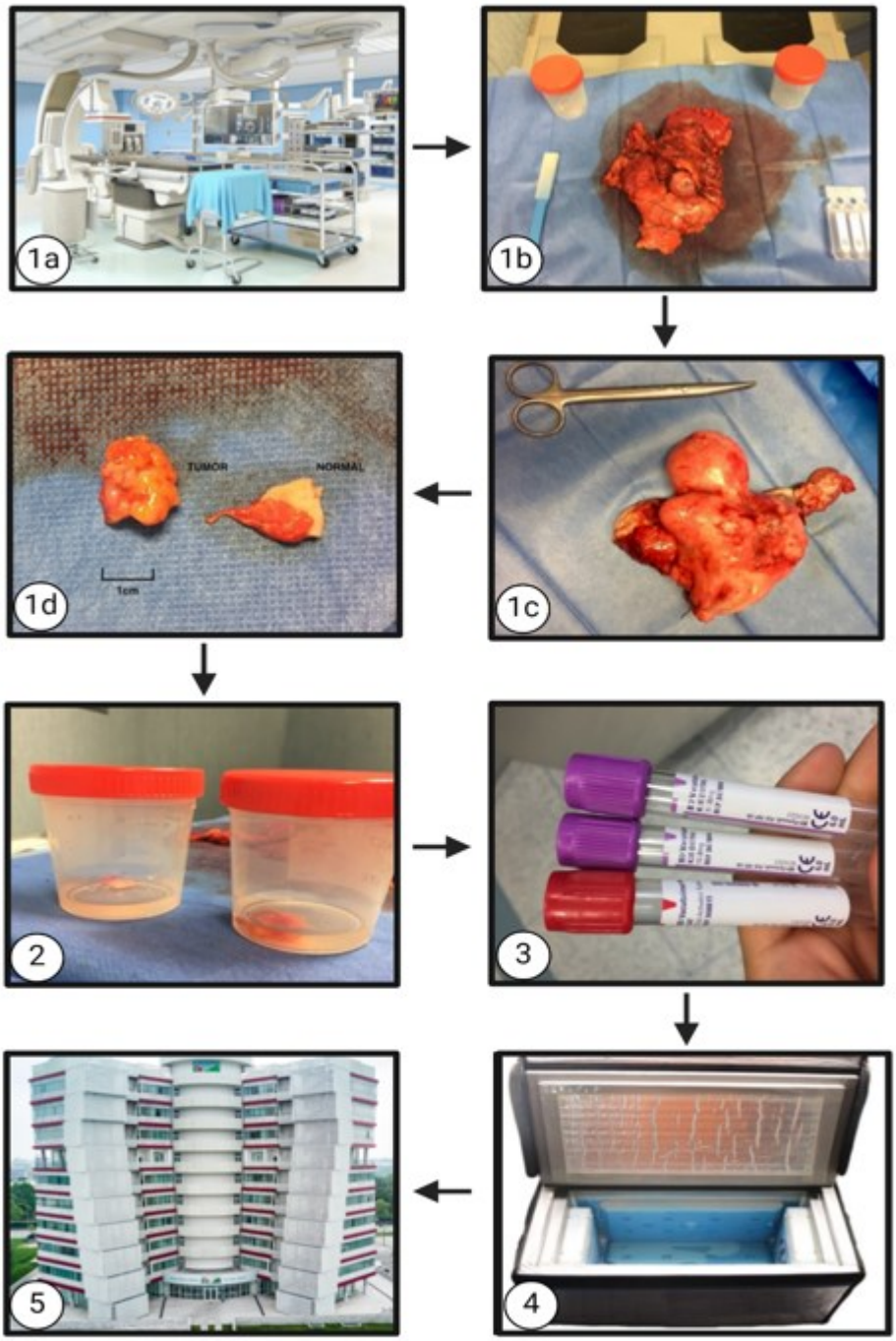

***Figure 10**: **Development of a standard operating procedure for the establishment of an OC CAFs biorepository**. (1a) OC surgery following standard clinical procedures, (1b) Specimen extraction, (1c) Ovary isolation, (1d) Biopsy, (2) Sample handling, (3) Arterial blood sampling, (4,5) Sample transport.*

4.2. CAFs derivation protocol

1. **Initial sample handling upon arrival in laboratory**: Wash the samples with a buffer solution composed of:
    a. DMEM/F12 (Gibco™)
    b. 1% HEPES (Gibco™)
    c. 1% Anti-anti (Gibco™, 100X)
    d. 1% P/S (Gibco™, v/v)
2. **Mechanical tissue digestion:**
    a. Mechanically process the washed samples to achieve uniform consistency.
    b. Transfer the homogenized samples into the wells of a 24-well plate.
3. **Enzymatic digestion:**
    a. Prepare a digestion mix composed of:
        i. DMEM/F12 (Gibco™)
        ii. 2% Liberase™ (ROCHE)
        iii. 1% Anti-anti (Gibco™, 100X)
        iv. 1% P/S (Gibco™, v/v)
        v. 0.1% ROCK inhibitor (v/v)
    b. Add an adequate volume of the digestion mix to completely cover the tissue pieces in the 24-well plate.
4. **Incubation**:
    a. Incubate the plate at 37°C for 1 hour, mixing the digestion solution every 15 minutes.
    b. Terminate the enzymatic reaction using the washing buffer.
5. **Centrifugation:** Transfer the mixture to a falcon tube and centrifuge at 1200 rpm for 5 minutes at 4°C.
6. **Filtration and pellet resuspension:**
    a. Resuspend the resulting pellet in a fresh washing medium.
    b. Filter the resuspended solution through a 100 μm sieve.

   c. Centrifuge the filtered solution again at 1200 rpm for 5 minutes at 4°C.

- **Hemolysis (if needed):**
  - Incubate pellet with hemolysis solution at 37°C for 3 minutes.
  - Neutralize the enzymatic reaction using the washing buffer.
  - Centrifuge at 1200 rpm for 5 minutes at 4°C.

7. **Transfer to culture flask:** Transfer the final pellet to a T25 flask containing 4 mL of culture medium composed of:
   a. DMEM/F12 (Gibco™)
   b. 10% FBS (v/v)
   c. 1% P/S (Gibco™, v/v)
8. **Incubation and culture maintenance:**
   a. Incubate the flask at 37°C for 48 hour.
   b. Replace the culture medium every 48 hours.
   c. Continue culturing the cells until they reach 85% confluence.

- **Subculture:**
  - Once cells reach 85% confluence, detach them using Trypsin-EDTA (0.025%) solution.
  - Subculture the cells into new flasks, changing the culture medium every two to three days.

The protocol is illustrated in Figure 11 and demonstrated in Figure 12.

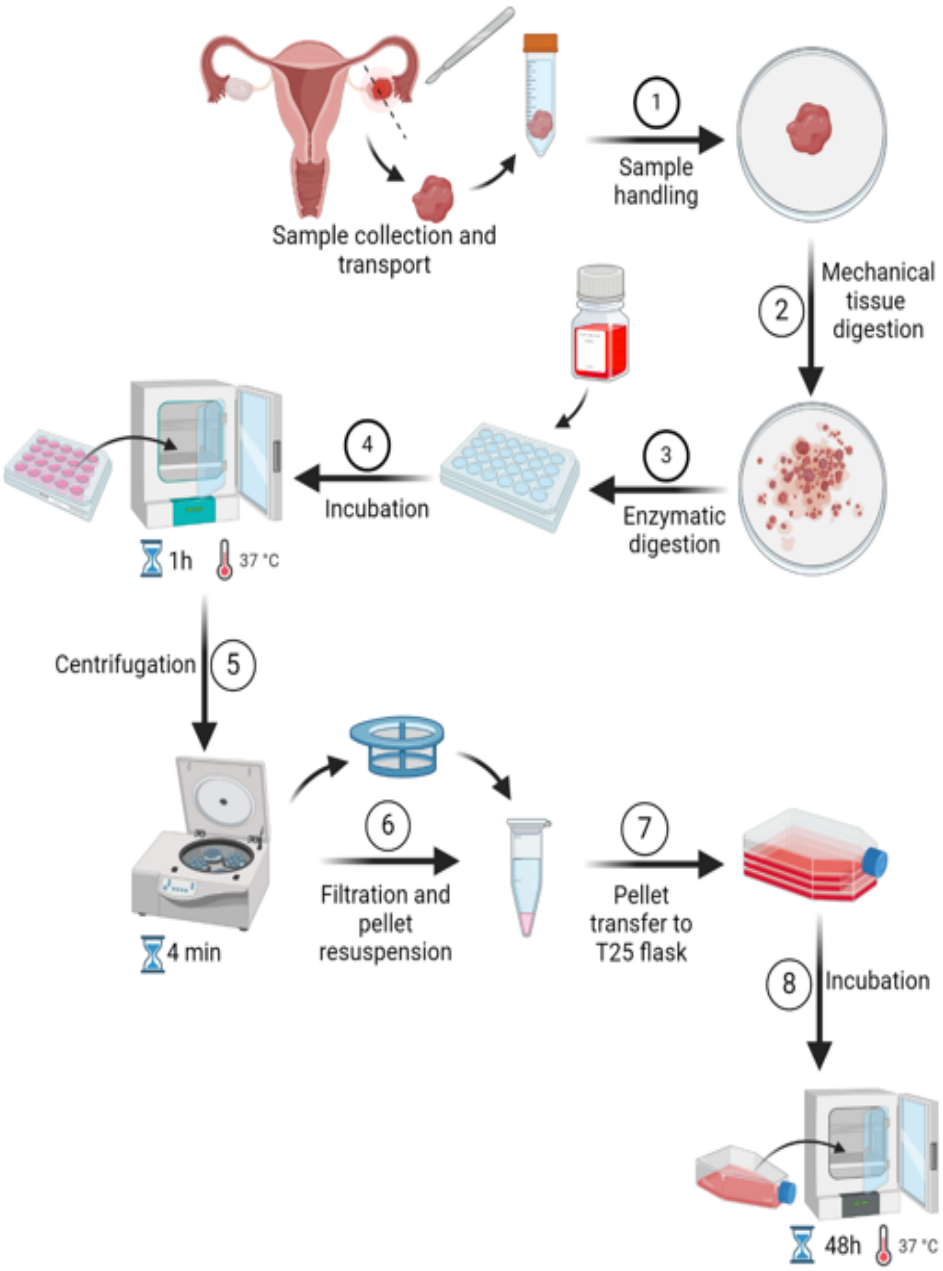

***Figure 11**: **Illustration of the CAFs derivation protocol**. After sample collection and transport: (1) Sample handling, (2) Mechanical tissue digestion, (3) Enzymatic digestion, (4) Incubation, (5) Centrifugation, (6) Filtration and pellet resuspension, (7) Pellet transfer, (8) Incubation.*

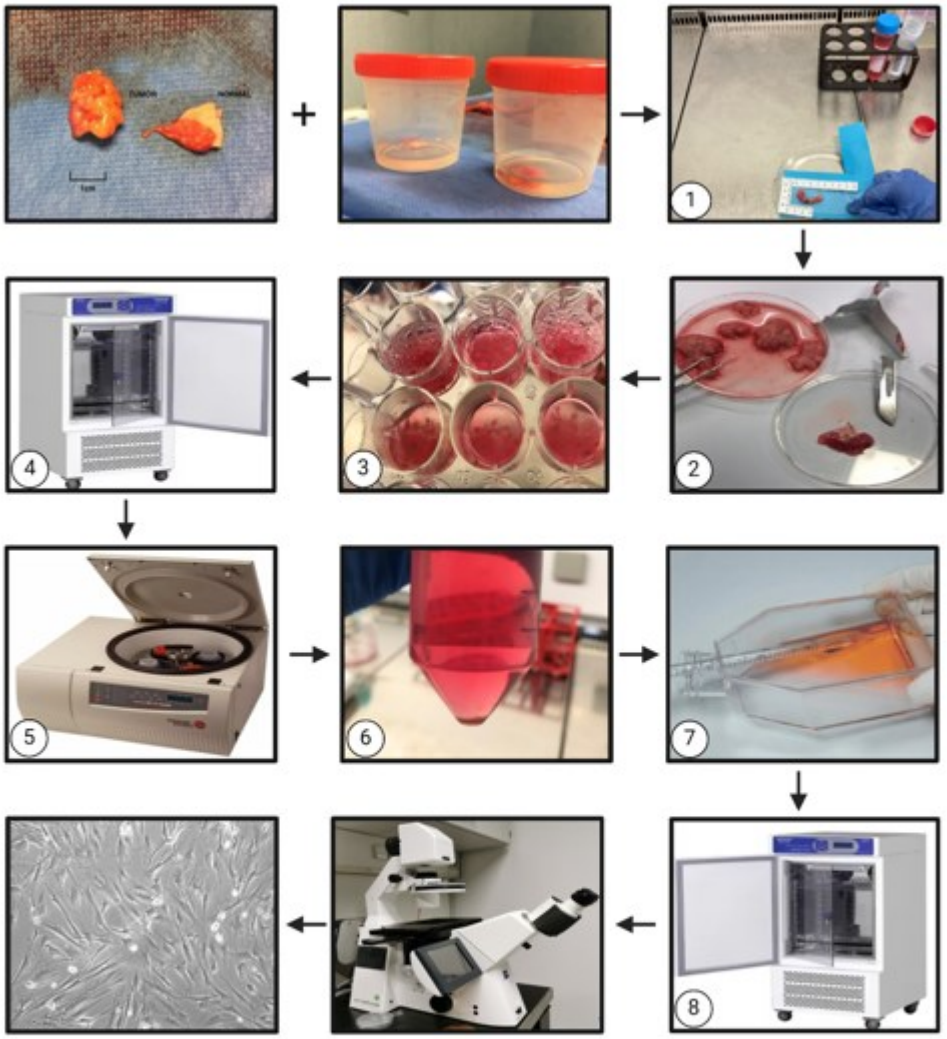

***Figure 12**: **Visualization of the CAFs derivation protocol**. After sample collection and transport: (1) Sample handling, (2) Mechanical tissue digestion, (3) Enzymatic digestion, (4) Incubation, (5) Centrifugation, (6) Filtration and pellet resuspension, (7) Pellet transfer, (8) Incubation. CAFs morphology can be observed using a Zeiss Axio Observer*

4.3. Characterization of HGSOC-derived CAFs: omental vs. primary tumor CAFs comparison

Following the derivation protocol, IF analysis was conducted to quantify the expression of key target proteins (CD29, FAP, and α-SMA) in CAF populations derived from both the primary tumor and the omentum. Microscopic images illustrating the qualitative characteristics of both populations are shown in Figure 13. Positive expression of CD29 (integrin β1) was observed in both populations. Additionally, both CAF populations exhibited positive expression of FAP, a type II integral serine protease. Lastly, α-SMA, a cytoplasmic microfilament protein, was similarly expressed in both populations. The blue nuclei in both populations are stained with Hoechst.

Notably, morphological differences between the two CAF populations were identified. In bright-field microscopy images of omental CAFs, the cells displayed a more rounded structure, in contrast to the spindle-shaped morphology observed in CAFs derived from the primary tumor.

The characterization is demonstrated in Figure 13.

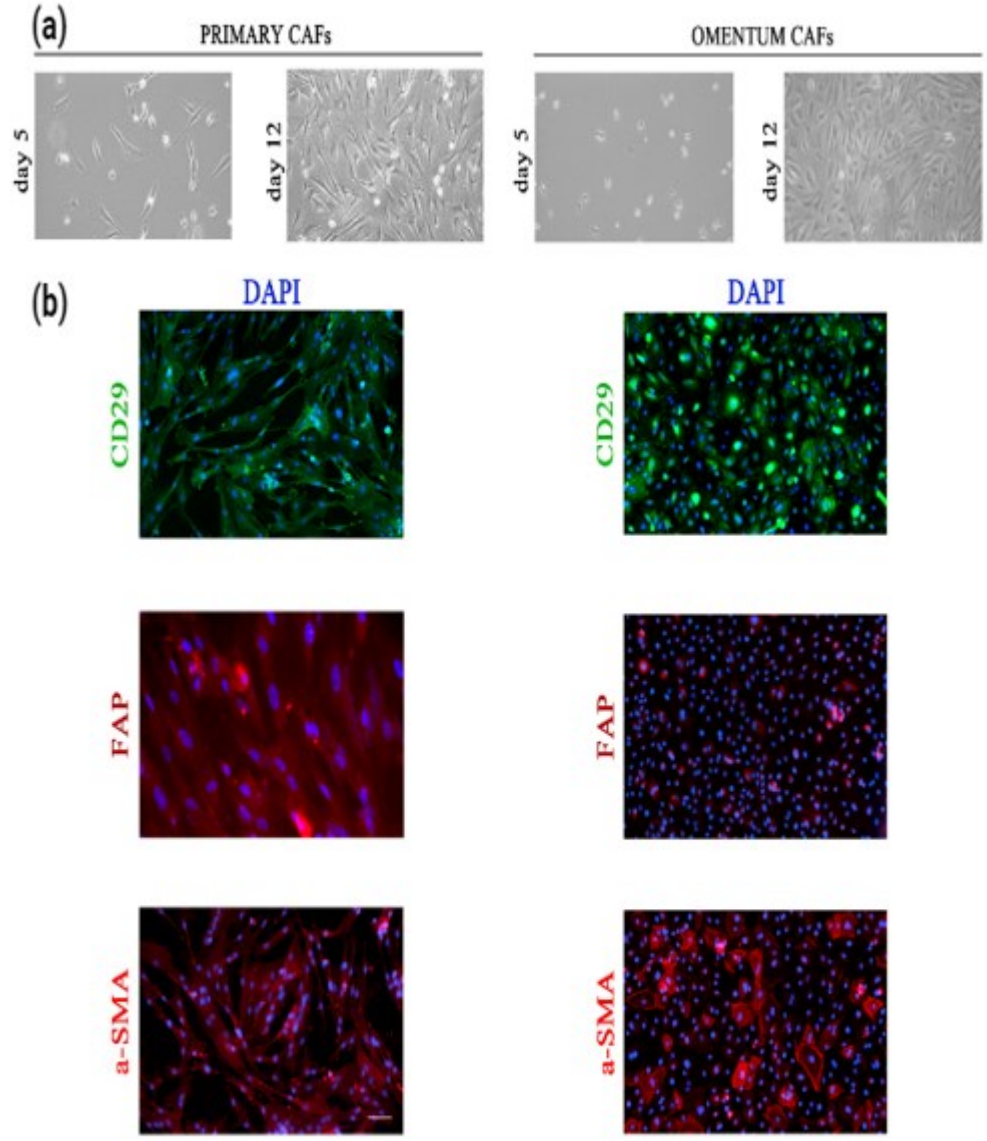

Figure 13: Bright-field microscopy and IF comparison if HGSOC CAFs from primary tumor (left) and omentum (right). *(a) Bright-field microscopy after 5 and 12 days of incubation. (b) IF analysis for three biomarkers: CD29 (green), FAP (upper red), α-SMA (lower red), and Hoechst counterstaining of nuclei (blue). Scale bar: 100 µm.*

4.4. Ki-67 proliferation analysis of OVCAR3 tumor cells, CAFs and their co-culture

IF analysis was conducted to evaluate and quantify the expression of Ki-67, a nuclear protein expressed during all phases of cell proliferation. This analysis was performed on three different groups: OVCAR3 tumor cells, CAFs, and a co-culture of CAFs and OVCAR3 tumor cells. The analysis is demonstrated in Figure 14.

In the OVCAR3 cell line, IF analysis revealed 70% Ki-67 positive cells. Staining for F-actin, in red, was conducted to observe cell morphology, revealing a rounded cellular shape, with nuclei stained blue by Hoechst

After 24 hours of culture, IF analysis was conducted on CAFs cultured alone and CAFs co-cultured with OVCAR3 tumor cells to assess their Ki-67 expression. The positive Ki-67 expression, displayed in the graph in Figure 14, was 5% for CAFs alone and 6.5% for CAFs in co-culture. Additionally, Figure 14 illustrates the morphological differences between CAFs and OVCAR3 tumor cells.

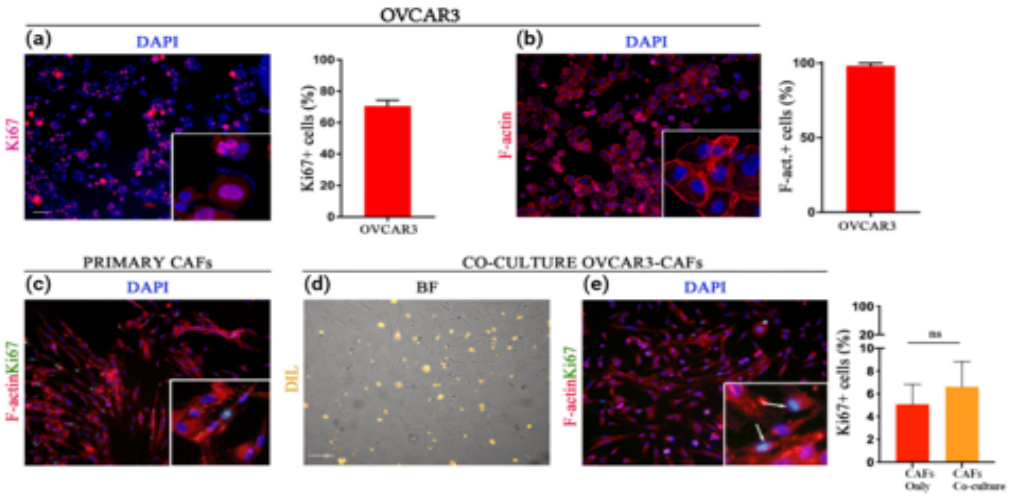

***Figure 14: Ki-67 Proliferation analysis**. The figure illustrates the IF analysis of three main groups and their relative quantification: OVCAR3, (a) Ki-67 (pink), (b) F-actin (red) and Hoechst counterstaining of nuclei (blue); Primory CAFs, (c) Ki-67 (turquoise), F-actin (red) and Hoechst counterstaining of nuclei (blue); OVCAR3-CAFs co-culture, (e) Ki-67 (turquoise), F-actin (red) and Hoechst counterstaining of nuclei (blue). Additionally, (d) Bright-field microscopy of co-culture of HGSOC CAFs and OVCAR3, with DIL counterstaining of nuclei (yellow). Scale bar: 100 µm.*

5. DISCUSSION

OC remains the most lethal gynecologic malignancy, with HGSOC being the most common and aggressive subtype, often diagnosed at advanced stages with peritoneal dissemination [2]. While patients initially respond to the combination of platinum-based agents and taxanes, most relapse due to chemoresistance contributing to over 90% of OC-related deaths [70]. A key factor in treatment failure is intratumor heterogeneity, as genetic diversity within a single tumor complicates therapeutic responses [12]. Studies suggest that a single biopsy may not fully capture a tumor's complexity, emphasizing the need for more comprehensive methods to assess intratumor heterogeneity [71,72]. Additionally, persistent genetic alterations and factors such as the ECM contribute to clonal diversity and resistance, making it essential to better understand chemoresistance mechanisms for advancing personalized medicine in OC [73].

Preclinical 2D and 3D models, such as cancer cell lines, PDXs, GEMMs and spheroids, are critical tools for studying tumor behavior. However, they frequently differ from the features of original malignancies [74]. PDXs retain tumor features in vivo but may lose heterogeneity and struggle to replicate human immune responses [19,28]. GEMMs provide insights into tumor biology but lack the complexity of human tumors [19,29]. While spheroids provide an environment closer to that of an in vivo setting they struggle simulating the intricate structure of tumors [30,31]. PDOs present a more advanced model, closely mimicking the genetic and phenotypic heterogeneity of original tumors, making them valuable for studying tumor evolution and drug sensitivity [19,37,38,73,75].

PDOs, as 3D in vitro reconstructions, provide a scalable and ethically favorable platform for personalized medicine and drug development [27,36]. PDOs encounter two key limitations: The absence of standardized protocols and the insufficient representation of the TME. The former affects various aspects of research, the sources and processing of cancer tissues, as well as the preparation of culture

media, which adds unpredictability and makes cross-study reproducibility more difficult [45]. The latter is essential for accurately modeling tumor behavior and treatment responses [45,76].

CAFs are diverse and important components of the TME and ECM, significantly influencing tumor progression [52,53,77]. Using proteolytic and mechanical mechanisms, CAFs actively alter cellular behavior to promote tumor proliferation and metastasis. Co-culturing CAFs with tumor cells has shown potential, as studies demonstrate that CAFs secrete growth factors, cytokines, and enzymes while promoting angiogenesis and EMT, which reshape the ECM [78-80]. By creating physical barriers that prevent the delivery of drugs and the infiltration of immune cells, they contribute to tumor chemoresistance [60]. Enhancing PDO models to better mimic the complex interactions within the TME, including CAF-driven ECM remodeling, could improve the predictive value of these systems [66].

In OC specifically, other challenges for PDOs include low incidence, tumor heterogeneity, and difficulties in deriving PDOs from dense tumors [19].

To further advance the filed in OC, we have developed a standardized protocol for the collection and preservation of OC tissues, necessary for maintaining the integrity and reproducibility of the sample. Using this protocol, the biological properties of the tissues are maintained and contamination is kept to a minimum, which guarantees sterile conditions and uniform sample processing. The addition of arterial blood samples for serum and plasma preservation improves the comprehensiveness, facilitating studies that use both tissue and blood-based biomarkers.

In this study, we successfully established a protocol for the derivation of CAFs from HGSOC samples. The process involved mechanical and enzymatic tissue digestion, followed by incubation and washing steps, yielding viable CAFs. The successful isolation of CAFs underscores the effectiveness of this protocol and suggests its potential for future standardization in CAF research. Additionally, we

successfully cultured HGSOC-derived CAFs in T25 flasks using a medium consisting of DMEM/F12, 10% FBS, and 1% P/S. The cells exhibited slow adhesion and proliferation rates, consistent with those reported in the literature [81,82]. Serum concentration is a critical factor in cell culture media, as FBS provides essential growth factors and nutrients necessary for supporting cell proliferation in vitro. Higher serum concentrations, such as 20%, are generally expected to promote faster cell growth compared to lower concentrations like 10% [83]. To accelerate the proliferation rate of CAFs, a potential future step could be increasing the FBS concentration from 10% to 20%. To validate this hypothesis, further research should be conducted, including an update of the current protocol to incorporate a 20% FBS medium, which may enhance proliferation and overall cell culture outcomes.

To investigate the phenotype of HGSOC-derived CAFs, we utilized bright-field microscopy to capture images on days 5 and 12 of culture from cells derived from both the primary tumor and the omentum. In the CAFs derived from the primary tumor, we observed large, flat, spindle-shaped cells with elongated processes extending from the cell body and a flat, oval nucleus. This phenotype aligns with the typical descriptions of CAFs found in the literature [84,85]. In contrast, CAFs derived from the omentum exhibited a more rounded cellular structure with fewer and less pronounced processes.

The identification and characterization of these cells as CAFs were confirmed through triple IF staining for CD29, FAP, and α-SMA, markers widely recognized in the literature as specific to CAFs [53,62–64]. CD29, also known as integrin β1, is a key surface protein involved in cell adhesion, signaling, and ECM interactions [86]. FAP, a type II integral serine protease expressed by activated fibroblasts [87]. The third marker, α-SMA, a cytoplasmic protein located in microfilament bundles, is characteristic of myofibroblasts [88]. These cells are crucial in fibrogenesis, utilizing cytoskeletal proteins for contraction and producing substantial ECM proteins

upon activation, contributing to the fibrotic response. All three marker expressions were positive in both the primary tumor and omental CAFs.

Comparing the IF images of these three markers, it is evident that the CAFs derived from the primary tumor exhibit an elongated spindle shape and nuclei, while the CAFs from the omentum display a more rounded shape with fewer cellular extensions. These characteristics are consistent with the ones observed in bright-field microscopy.

Ki-67 is a well-established biomarker for cell proliferation and a useful indicator of patient prognosis. It is expressed during the active phases of the cell cycle (G1, S, G2, and M) and is absent in quiescent cells (G0 phase) [89–91]. In this study, we used IF to evaluate the Ki-67 in three groups: the OVCAR3 cell line (a widely used model for OC), CAFs cultured alone, and CAFs co-cultured with OVCAR3 cells.

OVCAR3, exhibited Ki-67 expression of 70%, consistent with findings reported in the literature [92,93]. In addition, tumor cell adherence and morphology were analyzed using F-actin staining. F-actin is a major component of the cytoskeleton involved in cell motility, shape maintenance, and transcription regulation [94,95].

In contrast, CAFs cultured alone exhibited a Ki-67 expression of around 5%, a lower rate than reported in previous studies. This may be attributed to the low cell density resulting from the short incubation period, as suggested by the findings of M. Knops et al. In his study, it was demonstrated that CAFs with higher cell density exhibited significantly increased Ki-67 expression, indicating that cell proliferation is density-dependent [96].

We carried out a co-culture experiment to explore the complex cell-to-cell interactions between CAFs and OVCAR3. Such interactions are known to play a significant role in the TME, influencing both cancer progression and the behavior of stromal cells. After 24 hours, Ki-67 expression in the CAFs from the co-culture was 6.5%, which aligns with previous studies suggesting that the interaction between tumor cells and CAFs stimulate CAF proliferation [97].

Despite their slightly elevated Ki-67 expression, the CAFs proliferation in the co-culture was lower than anticipated. Several factors could explain the modest increase in Ki-67 in the co-culture. Our IF analysis was conducted after only 24 hours of co-culture. In previous works by J. Xu et al. and Hawsawi et al., CAFs were cultured for a longer period of time before the proliferation analysis (48h and 72h correspondingly), which provided them with more time to proliferate and form adhesions [98,99]. Additionally, as previously stated, FBS concentration may also be a contributing factor and should be increased in future experiments.

Other limitations to this work are the small sample size used, limiting the generalizability of the conclusions drawn, and the absence of ECM components in the experimental setup, which are essential for modulating CAF behavior and interactions with tumor cells.

Future works should prioritize the development of standardized protocols for the culture and derivation of CAFs in OC, improve reproducibility as well as render cross-study comparisons credible. Increasing sample sizes in future experiments will provide more robust data and improve the generalizability of findings. In addition, incorporating ECM components into experimental models is essential for understanding their influence on tumor cell behavior, such as proliferation and migration, which may reveal new therapeutic targets.

An interesting future direction could involve co-culturing CAFs with PDOs instead of traditional cell lines to create more accurate tumor models. Current in vitro methods, such as cell lines, may overestimate therapeutic efficacy. In contrast, 3D co-culture models of CAFs with PDOs offer more physiologically relevant interactions, better reflecting the TME and improving the accuracy of therapeutic evaluations.

6. CONCLUSIONS

The derivation and culture of CAFs from high-grade serous ovarian carcinoma samples resulted in viable cells, as confirmed by the immunofluorescence analyses. The cells displayed expected morphologies and expressed key markers, including CD29, FAP, and α-SMA. These findings indicate that, with further validation, the proposed protocol could become a reliable standardized method for the derivation of CAFs. A standardized approach would be beneficial for ensuring consistent results and advancing research on the role of CAFs in ovarian cancer.

Furthermore, the co-culture of CAFs with OVCAR3 tumor cells showed a slight increase in the expression of CAFs Ki-67 positive cells compared to CAFs cultured alone, suggesting a pro-proliferative interaction between the tumor cells and CAFs. This highlights the importance of CAF-tumor interactions in cancer progression and the potential for developing therapeutic approaches that target these interactions. Hence, focusing on the tumor microenvironment, and particularly on the role of CAFs, could lead to better models for studying ovarian cancer and improving treatment strategies.

7. REFERENCES

1. Yee C, Dickson KA, Muntasir MN, Ma Y, Marsh DJ. Three-Dimensional Modelling of Ovarian Cancer: From Cell Lines to Organoids for Discovery and Personalized Medicine. *Front Bioeng Biotechnol*. 2022;10:836984. doi:10.3389/fbioe.2022.836984
2. Torre LA, Trabert B, DeSantis CE, et al. Ovarian cancer statistics, 2018. *CA Cancer J Clin*. 2018;68(4):284-296. doi:10.3322/caac.21456
3. Surveillance, Epidemiology, and End Results (SEER) Program. U.S. Population Data 1969-2022. Published online March 2024. www.seer.cancer.gov/popdata
4. Barnes BM, Nelson L, Tighe A, et al. Distinct transcriptional programs stratify ovarian cancer cell lines into the five major histological subtypes. *Genome Med*. 2021;13(1):140. doi:10.1186/s13073-021-00952-5
5. Köbel M, Kang EY. The Evolution of Ovarian Carcinoma Subclassification. *Cancers*. 2022;14(2):416. doi:10.3390/cancers14020416
6. Kossaï M, Leary A, Scoazec JY, Genestie C. Ovarian Cancer: A Heterogeneous Disease. *Pathobiology*. 2018;85(1-2):41-49. doi:10.1159/000479006
7. Lheureux S, Braunstein M, Oza AM. Epithelial ovarian cancer: Evolution of management in the era of precision medicine. *CA Cancer J Clin*. 2019;69(4):280-304. doi:10.3322/caac.21559
8. Kurman RJ, Shih IM. The origin and pathogenesis of epithelial ovarian cancer: a proposed unifying theory. *Am J Surg Pathol*. 2010;34(3):433-443. doi:10.1097/PAS.0b013e3181cf3d79
9. Ramus SJ, Gayther SA. The Contribution of *BRCA1* and *BRCA2* to Ovarian Cancer. *Mol Oncol*. 2009;3(2):138-150. doi:10.1016/j.molonc.2009.02.001
10. Lawrence Impey, Tim Child. *Obstetrics and Gynaecology, 5th Edition*. 5th ed. Edra
11. Surveillance, Epidemiology, and End Results Program. Cancer Stat Facts: Ovarian Cancer. Published online 2021 2017. https://seer.cancer.gov/statfacts/html/ovary.html
12. Doubeni CA, Doubeni AR, Myers AE. Diagnosis and Management of Ovarian Cancer. *Am Fam Physician*. 2016;93(11):937-944.
13. Tardieu A, Ouldamer L, Margueritte F, et al. Assessment of Lymph Node Involvement with PET-CT in Advanced Epithelial Ovarian Cancer. A FRANCOGYN Group Study. *J Clin Med*. 2021;10(4):602. doi:10.3390/jcm10040602
14. Javadi S, Ganeshan DM, Qayyum A, Iyer RB, Bhosale P. Ovarian Cancer, the Revised FIGO Staging System, and the Role of Imaging. *Am J Roentgenol*. 2016;206(6):1351-1360. doi:10.2214/AJR.15.15199
15. Arora T, Mullangi S, Vadakekut ES, Lekkala MR. Epithelial Ovarian Cancer. In: *StatPearls*. StatPearls Publishing; 2024. Accessed May 21, 2024. http://www.ncbi.nlm.nih.gov/books/NBK567760/
16. Pepa CD, Tonini G, Pisano C, et al. Ovarian cancer standard of care: are there real alternatives? *Chin J Cancer*. 2015;34(1):17-27. doi:10.5732/cjc.014.10274

17. Aleksandra Kujawa K, Lisowska KM. Ovarian cancer – from biology to clinic. *Postępy Hig Med Dośw*. 2015;69:1275-1290. doi:10.5604/17322693.1184451
18. Wilczyński J, Paradowska E, Wilczyńska J, Wilczyński M. Prediction of Chemoresistance—How Preclinical Data Could Help to Modify Therapeutic Strategy in High-Grade Serous Ovarian Cancer. *Curr Oncol*. 2023;31(1):229-249. doi:10.3390/curroncol31010015
19. Spagnol G, Sensi F, De Tommasi O, et al. Patient Derived Organoids (PDOs), Extracellular Matrix (ECM), Tumor Microenvironment (TME) and Drug Screening: State of the Art and Clinical Implications of Ovarian Cancer Organoids in the Era of Precision Medicine. *Cancers*. 2023;15(7):2059. doi:10.3390/cancers15072059
20. Uner H, Demir M, Goksuluk D, Kars A, Uner M, Usubutun A. Evidence for diverse prognosis in high-grade serous ovarian carcinoma: solid, pseudoendometrioid, and transitional-like; so-called Â“set morphologyÂ” and progesterone receptor status. *Turk J Pathol*. Published online 2022. doi:10.5146/tjpath.2022.01571
21. Kleinmanns K, Bjørge L. Enhancing precision oncology in high-grade serous carcinoma: the emerging role of antibody-based therapies. *Npj Womens Health*. 2024;2(1):7. doi:10.1038/s44294-024-00010-6
22. Azzalini E, Stanta G, Canzonieri V, Bonin S. Overview of Tumor Heterogeneity in High-Grade Serous Ovarian Cancers. *Int J Mol Sci*. 2023;24(20):15077. doi:10.3390/ijms242015077
23. Soslow RA, Han G, Park KJ, et al. Morphologic patterns associated with BRCA1 and BRCA2 genotype in ovarian carcinoma. *Mod Pathol*. 2012;25(4):625-636. doi:10.1038/modpathol.2011.183
24. Kohn EC, Ivy SP. Whence High-Grade Serous Ovarian Cancer. *Am Soc Clin Oncol Educ Book*. 2017;(37):443-448. doi:10.1200/EDBK_174718
25. Takaya H, Nakai H, Takamatsu S, Mandai M, Matsumura N. Homologous recombination deficiency status-based classification of high-grade serous ovarian carcinoma. *Sci Rep*. 2020;10(1):2757. doi:10.1038/s41598-020-59671-3
26. Ngoi NYL, Tan DSP. The role of homologous recombination deficiency testing in ovarian cancer and its clinical implications: do we need it? *ESMO Open*. 2021;6(3):100144. doi:10.1016/j.esmoop.2021.100144
27. Dutta D, Heo I, Clevers H. Disease Modeling in Stem Cell-Derived 3D Organoid Systems. *Trends Mol Med*. 2017;23(5):393-410. doi:10.1016/j.molmed.2017.02.007
28. Van Weerden WM. Patient-Derived Xenograft Models in Cancer Research. *Cancers*. 2021;13(4):815. doi:10.3390/cancers13040815
29. Singh M, Murriel CL, Johnson L. Genetically Engineered Mouse Models: Closing the Gap between Preclinical Data and Trial Outcomes. *Cancer Res*. 2012;72(11):2695-2700. doi:10.1158/0008-5472.CAN-11-2786
30. Mittler F, Obeïd P, Rulina AV, Haguet V, Gidrol X, Balakirev MY. High-Content Monitoring of Drug Effects in a 3D Spheroid Model. *Front Oncol*. 2017;7:293. doi:10.3389/fonc.2017.00293
31. Jubelin C, Muñoz-Garcia J, Griscom L, et al. Three-dimensional in vitro culture

models in oncology research. *Cell Biosci*. 2022;12(1):155. doi:10.1186/s13578-022-00887-3
32. Botti G, Di Bonito M, Cantile M. Organoid biobanks as a new tool for pre-clinical validation of candidate drug efficacy and safety. *Int J Physiol Pathophysiol Pharmacol*. 2021;13(1):17-21.
33. Piccoli M, D'Angelo E, Crotti S, et al. Decellularized colorectal cancer matrix as bioactive microenvironment for in vitro 3D cancer research. *J Cell Physiol*. 2018;233(8):5937-5948. doi:10.1002/jcp.26403
34. Sokolova V, Rojas-Sánchez L, Białas N, Schulze N, Epple M. Calcium phosphate nanoparticle-mediated transfection in 2D and 3D mono- and co-culture cell models. *Acta Biomater*. 2019;84:391-401. doi:10.1016/j.actbio.2018.11.051
35. Ravi M, Paramesh V, Kaviya SR, Anuradha E, Solomon FDP. 3D Cell Culture Systems: Advantages and Applications. *J Cell Physiol*. 2015;230(1):16-26. doi:10.1002/jcp.24683
36. Xu H, Lyu X, Yi M, Zhao W, Song Y, Wu K. Organoid technology and applications in cancer research. *J Hematol OncolJ Hematol Oncol*. 2018;11(1):116. doi:10.1186/s13045-018-0662-9
37. Jabs J, Zickgraf FM, Park J, et al. Screening drug effects in patient-derived cancer cells links organoid responses to genome alterations. *Mol Syst Biol*. 2017;13(11):955. doi:10.15252/msb.20177697
38. Yang J, Huang S, Cheng S, Jin Y, Zhang N, Wang Y. Application of Ovarian Cancer Organoids in Precision Medicine: Key Challenges and Current Opportunities. *Front Cell Dev Biol*. 2021;9:701429. doi:10.3389/fcell.2021.701429
39. He X, Jiang Y, Zhang L, et al. Patient-derived organoids as a platform for drug screening in metastatic colorectal cancer. *Front Bioeng Biotechnol*. 2023;11:1190637. doi:10.3389/fbioe.2023.1190637
40. Wensink GE, Elias SG, Mullenders J, et al. Patient-derived organoids as a predictive biomarker for treatment response in cancer patients. *Npj Precis Oncol*. 2021;5(1):30. doi:10.1038/s41698-021-00168-1
41. Granat LM, Kambhampati O, Klosek S, Niedzwecki B, Parsa K, Zhang D. The promises and challenges of patient-derived tumor organoids in drug development and precision oncology. *Anim Models Exp Med*. 2019;2(3):150-161. doi:10.1002/ame2.12077
42. Zhao Z, Chen X, Dowbaj AM, et al. Organoids. *Nat Rev Methods Primer*. 2022;2(1):94. doi:10.1038/s43586-022-00174-y
43. Qu S, Xu R, Yi G, et al. Patient-derived organoids in human cancer: a platform for fundamental research and precision medicine. *Mol Biomed*. 2024;5(1):6. doi:10.1186/s43556-023-00165-9
44. Nanki Y, Chiyoda T, Hirasawa A, et al. Patient-derived ovarian cancer organoids capture the genomic profiles of primary tumours applicable for drug sensitivity and resistance testing. *Sci Rep*. 2020;10(1):12581. doi:10.1038/s41598-020-69488-9
45. Shi Y, Guan Z, Cai G, et al. Patient-derived organoids: a promising tool for breast cancer research. *Front Oncol*. 2024;14:1350935.

doi:10.3389/fonc.2024.1350935
46. Martin GR, Kleinman HK. Extracellular matrix proteins give new life to cell culture. *Hepatol Baltim Md*. 1981;1(3):264-266. doi:10.1002/hep.1840010312
47. Watters KM, Bajwa P, Kenny HA. Organotypic 3D Models of the Ovarian Cancer Tumor Microenvironment. *Cancers*. 2018;10(8):265. doi:10.3390/cancers10080265
48. Xu M, Zhang T, Xia R, Wei Y, Wei X. Targeting the tumor stroma for cancer therapy. *Mol Cancer*. 2022;21(1):208. doi:10.1186/s12943-022-01670-1
49. Frantz C, Stewart KM, Weaver VM. The extracellular matrix at a glance. *J Cell Sci*. 2010;123(24):4195-4200. doi:10.1242/jcs.023820
50. Nero C, Vizzielli G, Lorusso D, et al. Patient-derived organoids and high grade serous ovarian cancer: from disease modeling to personalized medicine. *J Exp Clin Cancer Res CR*. 2021;40(1):116. doi:10.1186/s13046-021-01917-7
51. Gargotti M, Lopez-Gonzalez U, Byrne HJ, Casey A. Comparative studies of cellular viability levels on 2D and 3D in vitro culture matrices. *Cytotechnology*. 2018;70(1):261-273. doi:10.1007/s10616-017-0139-7
52. Hedegaard CL, Redondo-Gómez C, Tan BY, Ng KW, Loessner D, Mata A. Peptide-protein coassembling matrices as a biomimetic 3D model of ovarian cancer. *Sci Adv*. 2020;6(40):eabb3298. doi:10.1126/sciadv.abb3298
53. Glabman RA, Choyke PL, Sato N. Cancer-Associated Fibroblasts: Tumorigenicity and Targeting for Cancer Therapy. *Cancers*. 2022;14(16):3906. doi:10.3390/cancers14163906
54. Chen Y, McAndrews KM, Kalluri R. Clinical and therapeutic relevance of cancer-associated fibroblasts. *Nat Rev Clin Oncol*. 2021;18(12):792-804. doi:10.1038/s41571-021-00546-5
55. Denton AE, Roberts EW, Fearon DT. Stromal Cells in the Tumor Microenvironment. In: Owens BMJ, Lakins MA, eds. *Stromal Immunology*. Vol 1060. Advances in Experimental Medicine and Biology. Springer International Publishing; 2018:99-114. doi:10.1007/978-3-319-78127-3_6
56. Mhawech-Fauceglia P, Yan L, Sharifian M, et al. Stromal Expression of Fibroblast Activation Protein Alpha (FAP) Predicts Platinum Resistance and Shorter Recurrence in patients with Epithelial Ovarian Cancer. *Cancer Microenviron*. 2015;8(1):23-31. doi:10.1007/s12307-014-0153-7
57. Yang D, Liu J, Qian H, Zhuang Q. Cancer-associated fibroblasts: from basic science to anticancer therapy. *Exp Mol Med*. 2023;55(7):1322-1332. doi:10.1038/s12276-023-01013-0
58. Deshmukh S, Dive A, Moharil R, Munde P. Enigmatic insight into collagen. J Oral Maxillofac Pathol. 2016;20(2):276. doi:10.4103/0973-029X.185932
59. Kadler KE, Baldock C, Bella J, Boot-Handford RP. Collagens at a glance. J Cell Sci. 2007;120(12):1955-1958. doi:10.1242/jcs.03453
60. Periostin: Novel diagnostic and therapeutic target for cancer. Histol Histopathol. 2007;(22):1167-1174. doi:10.14670/HH-22.1167
61. Lightner VA. Tenascin: Does It Play a Role in Epidermal Morphogenesis and Homeostasis? J Invest Dermatol. 1994;102(3):273-277. doi:10.1111/1523-1747.ep12371780

62. Nurmik M, Ullmann P, Rodriguez F, Haan S, Letellier E. In search of definitions: Cancer-associated fibroblasts and their markers. Int J Cancer. 2020;146(4):895-905. doi:10.1002/ijc.32193
63. Simon T, Salhia B. Cancer-Associated Fibroblast Subpopulations With Diverse and Dynamic Roles in the Tumor Microenvironment. Mol Cancer Res. 2022;20(2):183-192. doi:10.1158/1541-7786.MCR-21-0282
64. Givel AM, Kieffer Y, Scholer-Dahirel A, et al. miR200-regulated CXCL12β promotes fibroblast heterogeneity and immunosuppression in ovarian cancers. Nat Commun. 2018;9(1):1056. doi:10.1038/s41467-018-03348-z
65. Barbazán J, Matic Vignjevic D. Cancer associated fibroblasts: is the force the path to the dark side? Curr Opin Cell Biol. 2019;56:71-79. doi:10.1016/j.ceb.2018.09.002
66. Kay EJ, Koulouras G, Zanivan S. Regulation of Extracellular Matrix Production in Activated Fibroblasts: Roles of Amino Acid Metabolism in Collagen Synthesis. Front Oncol. 2021;11:719922. doi:10.3389/fonc.2021.719922
67. Wright K, Ly T, Kriet M, Czirok A, Thomas SM. Cancer-Associated Fibroblasts: Master Tumor Microenvironment Modifiers. Cancers. 2023;15(6):1899. doi:10.3390/cancers15061899
68. Anderson NM, Simon MC. The tumor microenvironment. Curr Biol. 2020;30(16):R921-R925. doi:10.1016/j.cub.2020.06.081
69. Bhattacharya A, Alam K, Roy NS, et al. Exploring the interaction between extracellular matrix components in a 3D organoid disease model to replicate the pathophysiology of breast cancer. J Exp Clin Cancer Res. 2023;42(1):343. doi:10.1186/s13046-023-02926-4
70. Li SS, Ma J, Wong AST. Chemoresistance in ovarian cancer: exploiting cancer stem cell metabolism. J Gynecol Oncol. 2018;29(2):e32. doi:10.3802/jgo.2018.29.e32
71. Schwarz RF, Ng CKY, Cooke SL, et al. Spatial and temporal heterogeneity in high-grade serous ovarian cancer: a phylogenetic analysis. PLoS Med. 2015;12(2):e1001789. doi:10.1371/journal.pmed.1001789
72. Zhang AW, McPherson A, Milne K, et al. Interfaces of Malignant and Immunologic Clonal Dynamics in Ovarian Cancer. Cell. 2018;173(7):1755-1769.e22. doi:10.1016/j.cell.2018.03.073
73. Liu HD, Xia BR, Jin MZ, Lou G. Organoid of ovarian cancer: genomic analysis and drug screening. Clin Transl Oncol. 2020;22(8):1240-1251. doi:10.1007/s12094-019-02276-8
74. Warren A, Chen Y, Jones A, et al. Global computational alignment of tumor and cell line transcriptional profiles. Nat Commun. 2021;12(1):22. doi:10.1038/s41467-020-20294-x
75. The Cancer Genome Atlas Research Network. Integrated genomic analyses of ovarian carcinoma. Nature. 2011;474(7353):609-615. doi:10.1038/nature10166
76. Podaza E, Kuo HH, Nguyen J, Elemento O, Martin ML. Next generation patient derived tumor organoids. Transl Res. 2022;250:84-97. doi:10.1016/j.trsl.2022.08.003
77. Yanes B, Rainero E. The Interplay between Cell-Extracellular Matrix

Interaction and Mitochondria Dynamics in Cancer. Cancers. 2022;14(6):1433. doi:10.3390/cancers14061433
78. Hughes CS, Postovit LM, Lajoie GA. Matrigel: a complex protein mixture required for optimal growth of cell culture. Proteomics. 2010;10(9):1886-1890. doi:10.1002/pmic.200900758
79. Kim S, Min S, Choi YS, et al. Tissue extracellular matrix hydrogels as alternatives to Matrigel for culturing gastrointestinal organoids. Nat Commun. 2022;13(1):1692. doi:10.1038/s41467-022-29279-4
80. Schuth S, Le Blanc S, Krieger TG, et al. Patient-specific modeling of stroma-mediated chemoresistance of pancreatic cancer using a three-dimensional organoid-fibroblast co-culture system. J Exp Clin Cancer Res. 2022;41(1):312. doi:10.1186/s13046-022-02519-7
81. Wu J, Fu R, Liu Z, et al. Cell proliferation downregulated by TGF-β2-triggered G1/S checkpoint in clinical CAFs. Cell Cycle. 2017;16(2):172-178. doi:10.1080/15384101.2016.1253641
82. Wen H, Nie Q, Jiang Z, Deng H. [Primary culture and characteristics of colorectal cancer-associated fibroblasts]. Zhonghua Bing Li Xue Za Zhi. 2015;44(10):719-724.
83. Kwon D, Kim JS, Cha BH, et al. The Effect of Fetal Bovine Serum (FBS) on Efficacy of Cellular Reprogramming for Induced Pluripotent Stem Cell (iPSC) Generation. Cell Transplant. 2016;25(6):1025-1042. doi:10.3727/096368915X689703
84. Gascard P, Tlsty TD. Carcinoma-associated fibroblasts: orchestrating the composition of malignancy. Genes Dev. 2016;30(9):1002-1019. doi:10.1101/gad.279737.116
85. Stylianou A, Gkretsi V, Stylianopoulos T. Transforming growth factor-β modulates pancreatic cancer associated fibroblasts cell shape, stiffness and invasion. Biochim Biophys Acta BBA - Gen Subj. 2018;1862(7):1537-1546. doi:10.1016/j.bbagen.2018.02.009
86. Leask A. Integrin β 1: A Mechanosignaling Sensor Essential for Connective Tissue Deposition by Fibroblasts. Adv Wound Care. 2013;2(4):160-166. doi:10.1089/wound.2012.0365
87. Xin L, Gao J, Zheng Z, et al. Fibroblast Activation Protein-α as a Target in the Bench-to-Bedside Diagnosis and Treatment of Tumors: A Narrative Review. Front Oncol. 2021;11:648187. doi:10.3389/fonc.2021.648187
88. Cherng, Shen and Young, Jenny and Ma, Hongbao. Alpha-smooth muscle actin (α-SMA). J AM Sci. 2008;4.
89. Davey MG, Hynes SO, Kerin MJ, Miller N, Lowery AJ. Ki-67 as a Prognostic Biomarker in Invasive Breast Cancer. Cancers. 2021;13(17):4455. doi:10.3390/cancers13174455
90. Zhylkibayev AA, Sarina NI, Mun EA, Eskendirova SZ. STANDARDIZATION OF KI-67 AS A BIOMARKER OF CELL PROLIFERATION. Eurasian J Appl Biotechnol. 2019;(2). doi:10.11134/btp.2.2019.1
91. Li LT, Jiang G, Chen Q, Zheng JN. Ki67 is a promising molecular target in the diagnosis of cancer (Review). Mol Med Rep. 2015;11(3):1566-1572. doi:10.3892/mmr.2014.2914

92. Sensi, Francesca, Spagnol, Giulia, Biccari, Andrea, et al. Patient-derived extracellular matrix from decellularized high-grade serous ovarian carcinoma tissues as a biocompatible support for organoids growth. Published online August 27, 2024.
93. Fontoura JC, Viezzer C, Dos Santos FG, et al. Comparison of 2D and 3D cell culture models for cell growth, gene expression and drug resistance. Mater Sci Eng C. 2020;107:110264. doi:10.1016/j.msec.2019.110264
94. Dominguez R, Holmes KC. Actin Structure and Function. Annu Rev Biophys. 2011;40(1):169-186. doi:10.1146/annurev-biophys-042910-155359
95. Von Der Ecken J, Müller M, Lehman W, Manstein DJ, Penczek PA, Raunser S. Structure of the F-actin–tropomyosin complex. Nature. 2015;519(7541):114-117. doi:10.1038/nature14033
96. Knops AM, South A, Rodeck U, et al. Cancer-Associated Fibroblast Density, Prognostic Characteristics, and Recurrence in Head and Neck Squamous Cell Carcinoma: A Meta-Analysis. Front Oncol. 2020;10:565306. doi:10.3389/fonc.2020.565306
97. Kobayashi H, Gieniec KA, Lannagan TRM, et al. The Origin and Contribution of Cancer-Associated Fibroblasts in Colorectal Carcinogenesis. Gastroenterology. 2022;162(3):890-906. doi:10.1053/j.gastro.2021.11.037
98. Xu J, Fang Y, Chen K, et al. Single-Cell RNA Sequencing Reveals the Tissue Architecture in Human High-Grade Serous Ovarian Cancer. Clin Cancer Res. 2022;28(16):3590-3602. doi:10.1158/1078-0432.CCR-22-0296
99. Hawsawi NM, Ghebeh H, Hendrayani SF, et al. Breast Carcinoma–Associated Fibroblasts and Their Counterparts Display Neoplastic-Specific Changes. Cancer Res. 2008;68(8):2717-2725. doi:10.1158/0008-5472.CAN-08-0192

8. RINGRAZIAMENTI

I would like to express my deepest gratitude to my husband, who has been my partner in every step of this journey. Your unwavering support and encouragement mean the world to me.

To my family, thank you for always being there, no matter the circumstances. Your love and understanding have carried me through even the toughest moments.

And to my cats, who always made me laugh.

"We are the champions, my friends
And we'll keep on fighting till the end
We are the champions
We are the champions
No time for losers
'Cause we are the champions of the World!"

Queen, 1977